Biphenyl heterocyclic fluorochrome sensor for rapid hydrazine detection: Design, synthesis, single crystal XRD and DFT studies

*Dinkal V. Kasundra, Rajamouli Boddula and Paresh N. Patel**

Laboratory of Bio-Organic Chemistry, Tarsadia Institute of Chemical Science (TICS),

Uka Tarsadia University, Bardoli – 394 350, Gujarat, India

**e-mail: pareshn111@yahoo.com*

S1. Materials and Methods:

All the chemicals were obtained from Sigma–Aldrich, TCI, Spectrochem and were used without further purification. Hydrazine hydrate and all spectroscopic grade solvents were purchased from Spectrochem. Solvents were dried over molecular sieves if necessary. The ^{1}H NMR spectra was recorded in $CDCl_3$ or DMSO-d6 at room temperature using a Bruker AVANCE III 400 MHz (AV 400) multi nuclei solution NMR Spectrometer, TMS was used as internal reference. ^{13}C NMR spectra was measured on Bruker AVANCE III 100 MHz (AV 100) with complete proton decoupling. Chemical shifts were reported in ppm from the TMS as an internal standard. HR–MS data were obtained in acetonitrile, with Thermo Scientific Orbitrap Elite Mass spectrometer. The UV-1900i SHIMADZU UV-spectrophotometer with quartz cuvette was used to measure steady-state UV visible absorption (path length: 1 cm). The spectrofluorometer (RF 6000 SHIMADZU) was used to detect steady-state fluorescence. Melting point is measured by open capillary method using Sigma Melting Point Apparatus. For thin layer chromatography (TLC) analysis throughout this work, Merck precoated TLC plates (silica gel 60 GF254, 0.25 mm) were used. The products were purified by recrystallization or column chromatography silica gel 60 (Merck, 230-400 mesh).

S2. Spectral data:

S2.1 (E)-1-([1,1'-biphenyl]-4-yl)-3-(pyridin-2-yl) prop-2-en-1-one (3a)

Light Yellow solid (74/87% KOH/Pyrrolidine), MP 249.68 °C; FT-IR (Bands cm^{-1}): 1730 (C=O),1687, 1284, 1104; ^{1}H NMR (400 MHz, DMSO) δ ppm: 8.75 – 8.70 (d, *J= 20* Hz, 1H), 8.26 – 8.19 (m, 3H), 7.95 – 7.87 (m, 4H), 7.81 – 7.75 (m, 3H), 7.56 – 7.51 (m, 2H), 7.47 (dd, *J* = 8.7, 2.3 Hz, 2H);^{13}C NMR (100 MHz, DMSO) δ ppm:189.41(C=O), 153.25, 150.55, 145.22, 143.49, 139.32, 137.71, 136.60, 129.77, 129.60, 128.95, 127.59, 127.51, 125.62, 125.51, 125.35; HRMS (ESI) *m/z:* $[M+H]^{+1}$ calculated for $C_{20}H_{15}NO$, 286.1254; found, 286.1232.

S2.2 (E)-1-([1,1'-biphenyl]-4-yl)-3-(pyridin-3-yl) prop-2-en-1-one (3b)

Light Yellow solid (75/86% KOH/Pyrrolidine), MP 249.68 °C; FT-IR (Bands cm^{-1}): 1730 (C=O), 1687, 1284, 1104; ^{1}H NMR (400 MHz, DMSO) δ ppm: 8.74 – 8.71 (d, *J*= 20 Hz, 1H), 8.24 – 8.20

(m, 3H), 7.95 – 7.88 (m, 4H), 7.80 – 7.76 (m, 3H), 7.55 – 7.51 (m, 2H), 7.47 (dd, *J* = 8.7, 2.3 Hz, 2H); ^{13}C NMR (100 MHz, DMSO) δ ppm: 198.47 (C=O), 150.04, 145.08, 139.31, 135.87, 130.13, 129.57, 129.48, 129.29, 129.18, 129.09, 128.90, 127.48, 127.38, 127.31, 127.06, 126.49, 126.35, 125.78, 123.81, 75.27; HRMS (ESI) *m/z:* [M+H] $^{+1}$ calculated for $C_{20}H_{15}NO$, 286.1254; found, 286.1232.

S2.3 (E)-1-([1,1'-biphenyl]-4-yl)-3-(pyridin-4-yl) prop-2-en-1-one (3c)

Yellow solid (78/88 % KOH/Pyrrolidine), MP 249.68 °C; FT-IR (Bands cm^{-1}): 1730 (C=O), 1687, 1284, 1104; ^{1}H NMR (500 MHz, $CDCl_3$) δ ppm: 9.05 (d, *J* = 15.4 Hz, 1H), 8.61 (d, *J* = 9.3 Hz, 1H), 8.48 (d, *J* = 8.1 Hz, 1H), 8.30 – 8.20 (m, 5H), 8.17 (d, *J* = 8.9 Hz, 1H), 8.13 – 8.03 (m, 1H), 7.90 (d, *J* = 15.4 Hz, 1H), 7.81 (d, *J* = 8.4 Hz, 1H), 7.73 – 7.68 (m, 1H), 7.58 – 7.25 (m, 2H); ^{13}C NMR (125 MHz, $CDCl_3$) δ ppm: 189.67 (C=O), 145.59, 141.41, 140.00, 137.14, 132.99, 131.35, 130.77, 130.42, 129.23, 128.99, 128.84, 128.76, 128.24, 127.37, 127.33, 126.35, 126.09, 125.95, 125.07, 125.04, 124.65, 124.26, 123.99, 122.65; HRMS (ESI) *m/z:* [M+H] $^{+1}$ calculated for $C_{20}H_{15}NO$, 286.1254; found, 286.1232.

S2.4 (E)-1-([1,1'-biphenyl]-4-yl)-3-(thiophen-2-yl) prop-2-en-1-one (3d)

Yellow solid (79/89 % KOH/Pyrrolidine), MP 253.08 °C; FT-IR (Bands cm^{-1}): 1730 (C=O), 1687, 1284; ^{1}H NMR (500 MHz, DMSO) δ ppm: 8.22 – 8.19 (d, *J* = 15 Hz, 2H), 7.96 (d, *J* = 15.3 Hz, 1H), 7.89 – 7.87 (d, *J* = 10 Hz, 2H), 7.82-7.83 (d, 1H), 7.83 – 7.77 (m, 2H), 7.74 (d, *J* = 3.5 Hz, 1H), 7.64 (d, *J* = 15.3 Hz, 1H), 7.54 (t, *J* = 7.6 Hz, 2H), 7.48 – 7.43 (m, 1H), 7.22 (dd, *J* = 5.0, 3.6 Hz, 1H); ^{13}C NMR (125 MHz, DMSO) δ ppm: 188.60 (C=O), 144.96, 140.22, 137.21, 133.43, 131.10, 129.66, 127.51, 120.87; HRMS (ESI) *m/z:* [M+H] $^{+1}$ calculated for $C_{19}H_{14}OS$, 291.0865; found, 291.0843.

S2.5 (E)-1-([1,1'-biphenyl]-4-yl)-3-(furan-2-yl) prop-2-en-1-one (3e)

Yellow solid (78/86 % KOH/Pyrrolidine), MP 196.2 °C; FT-IR (Bands cm^{-1}): 1730 (C=O), 1687, 1284; ^{1}H NMR (400 MHz, DMSO) δ ppm: 8.17 (d, *J* = 8.3 Hz, 1H), 8.07 (t, *J* = 8.4 Hz, 1H), 7.95 (s, 1H), 7.86 (dd, *J* = 15.0, 8.3 Hz, 2H), 7.78 (dd, *J* = 12.3, 5.0 Hz, 2H), 7.61 (s, 2H), 7.56 – 7.42 (m, 3H), 7.15 (d, *J* = 3.4 Hz, 1H), 6.72 (dd, *J* = 3.4, 1.7 Hz, 1H); ^{13}C NMR (100 MHz, DMSO) δ ppm: 188.53 (C=O), 151.65, 146.75, 144.94, 139.38, 136.80, 130.94, 129.59, 129.54, 128.89, 127.52, 127.48, 119.19, 117.62, 113.66; HRMS (ESI) *m/z:* [M+H] $^{+1}$ calculated for $C_{19}H_{14}O_2$, 275.1094; found, 275.1071.

S2.6 (E)-1-([1,1'-biphenyl]-4-yl)-3-(1H-imidazol-2-yl) prop-2-en-1-one (3f)

Yellow solid (77/86 % KOH/Pyrrolidine), MP 306.04 °C; FT-IR (Bands cm^{-1}): 1730 (C=O), 1687, 1284, 1104; ^{1}H NMR (400 MHz, DMSO) δ ppm: 8.17 (d, *J* = 8.3 Hz, 1H), 8.07 (d, *J* = 8.4 Hz, 1H), 7.95 (s, 1H), 7.86 (dd, *J* = 15.0, 8.3 Hz, 2H), 7.78 (dd, *J* = 12.3, 5.0 Hz, 2H), 7.61 (s, 2H), 7.56 – 7.42 (m, 3H), 7.15 (d, *J* = 3.4 Hz, 1H), 6.72 (dd, *J* = 3.4, 1.7 Hz, 1H); ^{13}C NMR (101 MHz, DMSO) δ ppm: 189.07 (C=O), 145.06, 144.04, 142.63, 139.73, 139.44, 136.96, 134.38, 130.16, 129.85, 129.72, 129.63, 129.56, 129.52, 127.61, 127.56, 127.51, 127.27, 127.13, 127.05, 125.89, 122.48, 113.51, 106.03; HRMS (ESI) *m/z:* $[M+H]^{+1}$ calculated for $C_{18}H_{14}N_2O$, 275.1106; found, 275.1184.

S2.7 (E)-1-([1,1'-biphenyl]-4-yl)-3-(benzo[b]thiophen-2-yl) prop-2-en-1-one (3g)

Yellow solid (73/83 % KOH/Pyrrolidine), MP 343.38 °C; FT-IR (Bands cm^{-1}): 1730 (C=O), 1687, 1284; ^{1}H NMR (400 MHz, $CDCl_3$) δ ppm: 8.13 – 8.10 (d, *J*= 4, 4 Hz, 2H), 8.06 (dd, *J* = 15.2, 0.5 Hz, 1H), 7.85 – 7.78 (m, 2H), 7.76 – 7.73 (dd, *J*= 4, 3.6 Hz, 2H), 7.69 – 7.64 (m, 2H), 7.59 (s, 1H), 7.52 – 7.45 (m, 3H), 7.44 – 7.36 (m, 3H); ^{13}C NMR (100 MHz, $CDCl_3$) δ ppm: 189.09 (C=O), 145.74, 140.35, 140.26, 139.93, 139.74, 137.61, 136.66, 129.96, 129.13, 129.00, 128.27, 127.37, 127.33, 126.50, 124.98, 124.58, 123.03, 122.53; HRMS (ESI) *m/z:* $[M+H]^{+1}$ calculated for $C_{23}H_{16}OS$, 341.1022; found, 341.1000.

S2.8 (E)-1-([1,1'-biphenyl]-4-yl)-3-(benzo[b]thiophen-3-yl) prop-2-en-1-one (3h)

Yellow solid (73/83 % KOH/Pyrrolidine), MP 343.38 °C; FT-IR (Bands cm^{-1}): 1730 (C=O), 1687, 1284, 1104; ^{1}H NMR (400 MHz, DMSO) δ ppm: 8.70 (s, 1H), 8.27 (t, *J* = 8.9 Hz, 3H), 8.15 – 8.08 (m, 3H), 7.91 (d, *J* = 8.6 Hz, 2H), 7.81 (dd, *J* = 8.3, 1.2 Hz, 2H), 7.59 – 7.42 (m, 5H); ^{13}C NMR (100 MHz, $CDCl_3$) δ ppm: 189.84 (C=O), 145.61, 140.61, 139.96, 137.38, 136.93, 136.33, 132.43, 129.13, 129.00, 128.71, 128.26, 127.36, 127.32, 125.20, 125.11, 123.12, 122.42, 122.26; HRMS (ESI) *m/z:* $[M+H]^{+1}$ calculated for $C_{23}H_{16}OS$, 341.1148; found, 341.1126.

S2.9 3-([1,1'-biphenyl]-4-yl)-5-(benzo[b]thiophen-2-yl)-4,5-dihydro-1H-pyrazole (3g-NH_2NH_2)

White solid (74%), MP above 300 °C; FT-IR (Bands cm^{-1}): 1100 (C-N), 1687, 1284; ^{1}H NMR (500 MHz, $CDCl_3$) δ ppm: 7.84 (d, J = 8.3 Hz, 2H), 7.73 (d, J = 7.9 Hz, 1H), 7.68 (t, J = 7.6 Hz, 3H), 7.65 – 7.60 (m, 2H), 7.47 (t, J = 7.6 Hz, 2H), 7.40 (d, J = 7.3 Hz, 1H), 7.34 – 6.04 (m, 2H), 6.00 (dd, J = 11.5, 4.1 Hz, 1H), 3.80 (dd, J = 17.5, 11.5 Hz, 1H), 3.46 (dd, J = 17.5, 4.1 Hz, 1H), 2.46 (s, 2H); HRMS (ESI) *m/z:* $[M+H]^{-1}$ calculated for $C_{23}H_{18}N_2S$, 353.1291; found, 353.1233.

S3. Crystal data:

Identification code	3g (CCDC: 2374118)
Empirical formula	$C_{23}H_{16}OS$
Formula weight	340.4400
Temperature	150 K
Wavelength	0.71073 Å
Crystal system	Monoclinic
Space group	P 1 21/c 1
Unit cell dimensions	a =12.7179(9) Å; a = 90° b = 5.4952(5) Å; b = 95.501(7) ° c = 24.4339(18) Å; c = 90°
Volume	1699.8(2) $Å^3$
Z	4
Density (calculated)	1.330 g/Cm^{-3}
Absorption coefficient	0.197 mm^{-1}
F (000)	712.0
Crystal size	0.3 x 0.2 x 0.15 mm^3
Theta range for data collection	0.999 to 24.999°
Index ranges	-15<=h<=15, -6<=k<=6, -29<=l<=29
Reflections collected	0.1381(1455)
Independent reflections	1455 [R(int) = 0.1381]
Completeness to theta = 24.998°	99.03 %
Absorption correction	MULTI-SCAN
Max. and min. transmission	1.000 and 0.100
Refinement method	Full-matrix least-squares on F^2
Data / restraints / parameters	3783 / 1635 / 416
Goodness-of-fit on F^2	0.999
Final R indices [I>2sigma(I)]	R1 = 0.0400, wR2 = 0.0769
R indices (all data)	R1 = 0.1381, wR2 = 0.4062
Extinction coefficient	n/a
Largest diff. peak and hole	0.131 and -0.161 e. $Å^{-3}$

S4. Spectrum of prepared molecules:

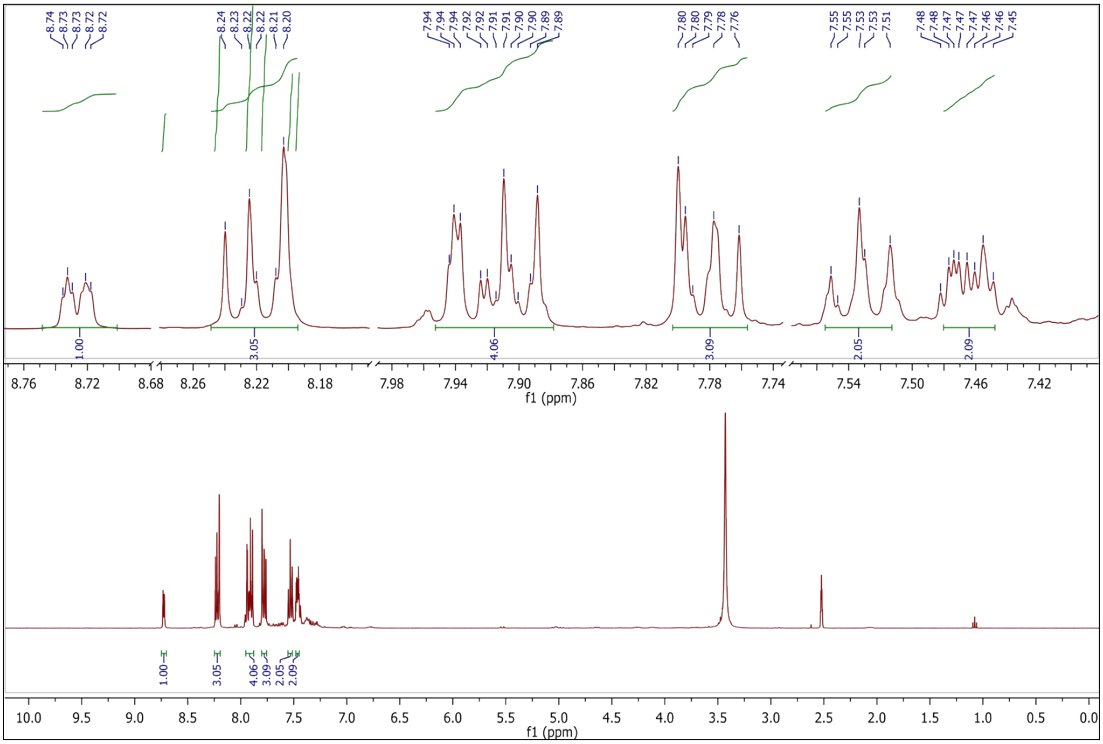

Figure S$_1$: ^{1}H NMR of *(E)*-1-([1,1'-biphenyl]-4-yl)-3-(pyridin-2-yl) prop-2-en-1-one (3a)

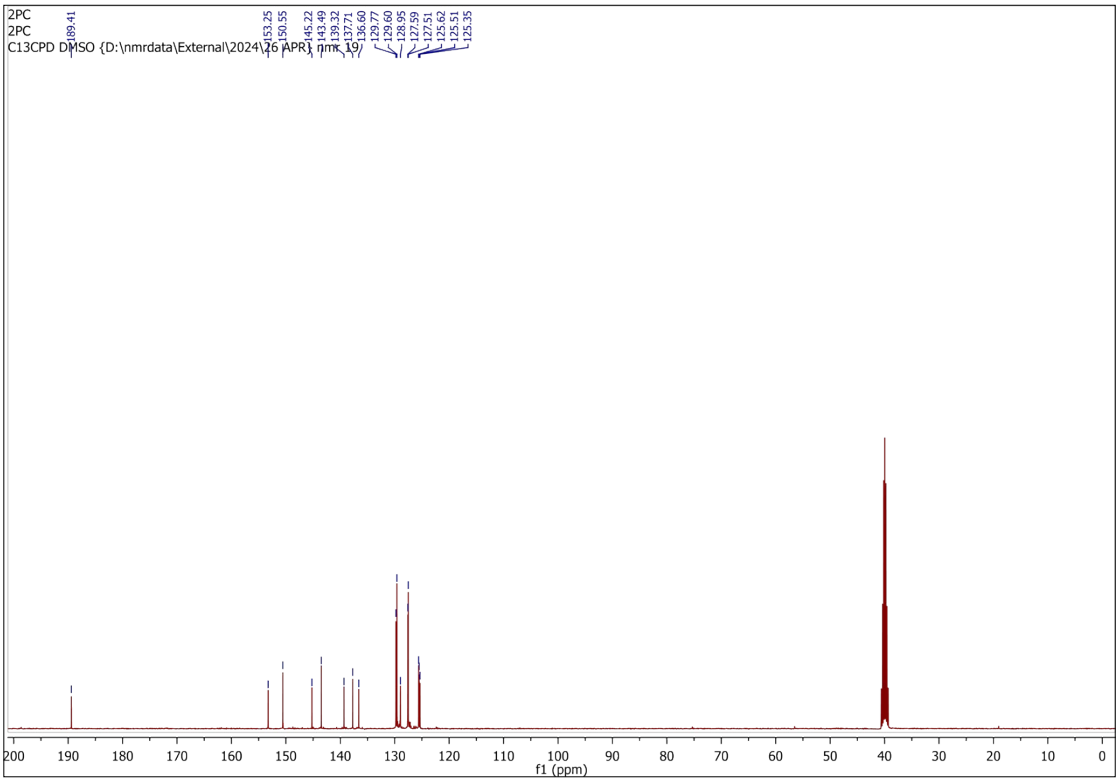

Figure S$_2$: ^{13}C NMR of *(E)*-1-([1,1'-biphenyl]-4-yl)-3-(pyridin-2-yl) prop-2-en-1-one (3a)

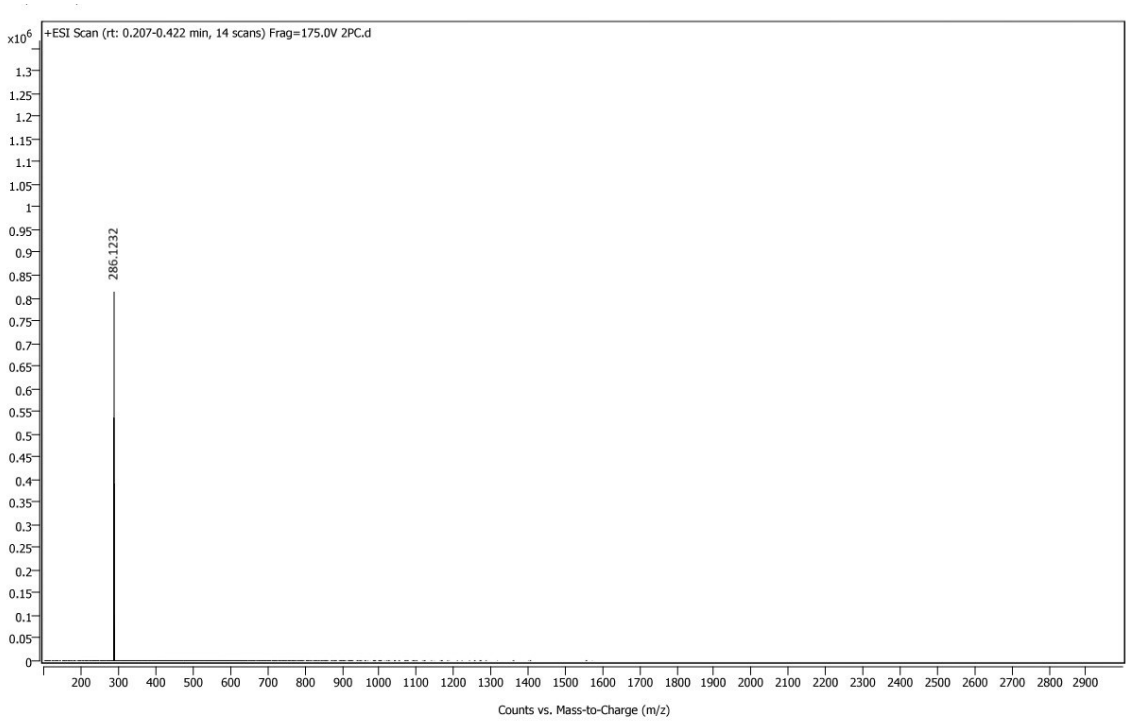

Figure S$_3$: HRMS of *(E)*-1-([1,1'-biphenyl]-4-yl)-3-(pyridin-2-yl) prop-2-en-1-one (3a)

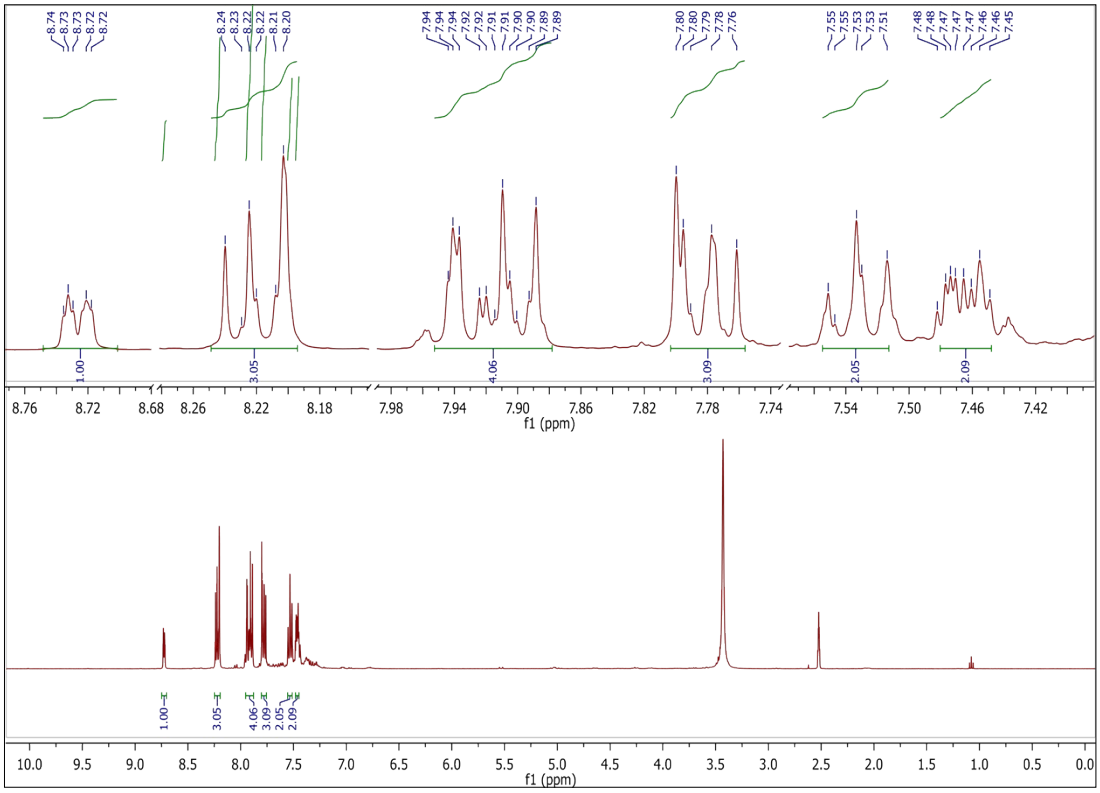

Figure S$_4$: ^{1}H NMR of *(E)*-1-([1,1'-biphenyl]-4-yl)-3-(pyridin-3-yl) prop-2-en-1-one (3b)

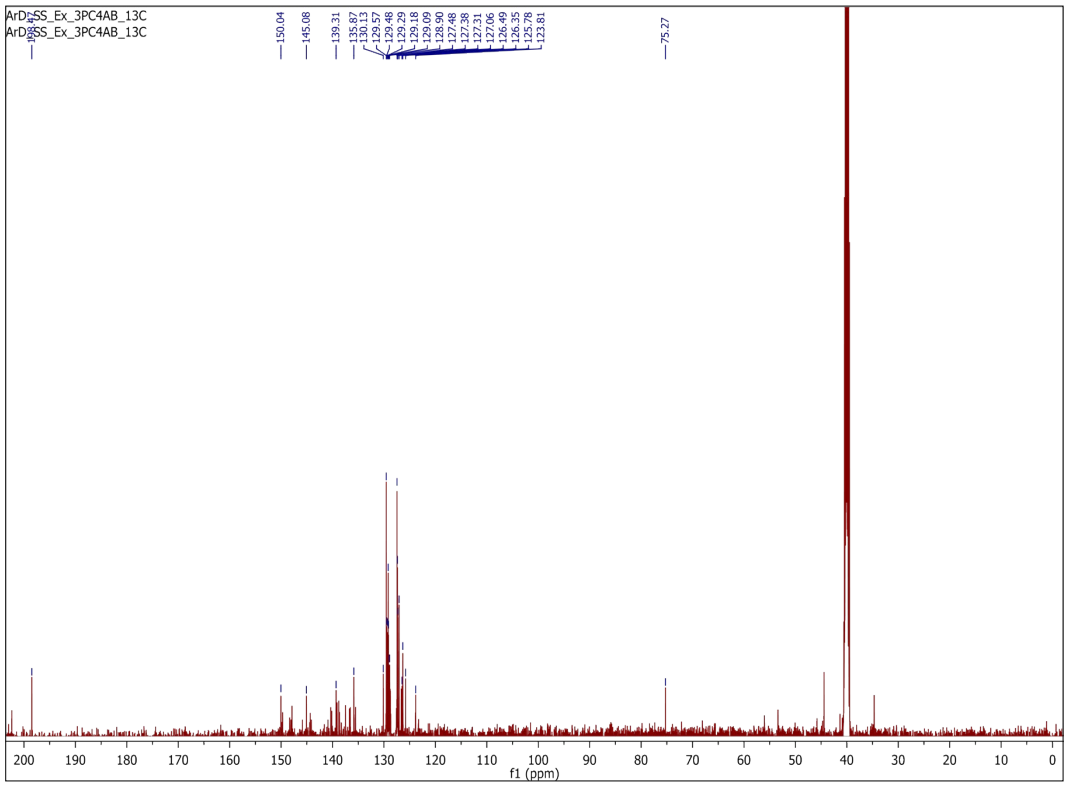

Figure S5: ^{13}C NMR of *(E)*-1-([1,1'-biphenyl]-4-yl)-3-(pyridin-3-yl) prop-2-en-1-one (3b)

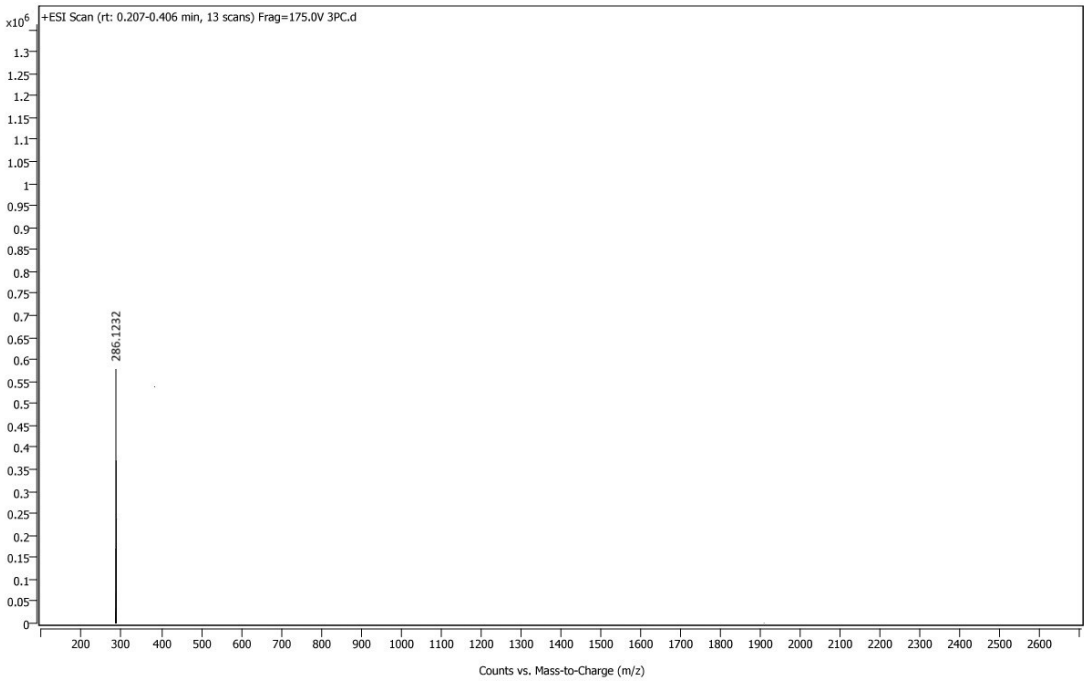

Figure S6: HRMS of *(E)*-1-([1,1'-biphenyl]-4-yl)-3-(pyridin-3-yl) prop-2-en-1-one (3b)

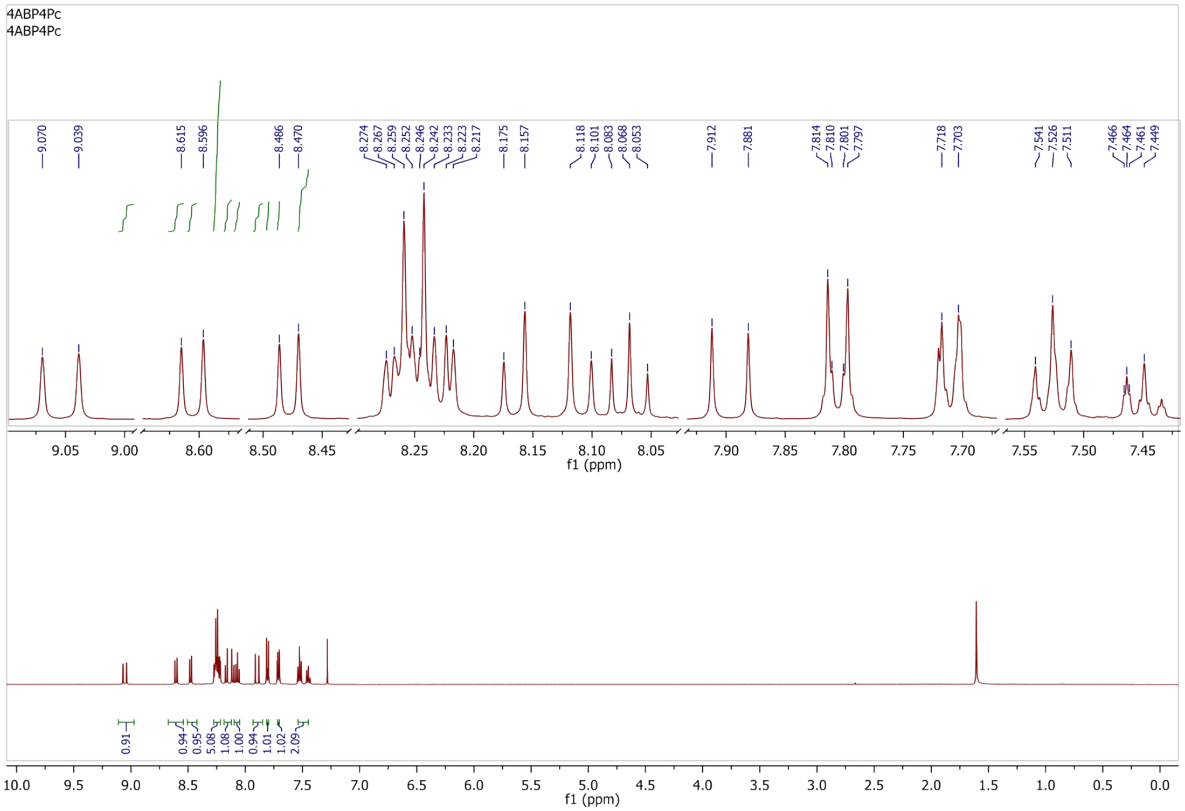

Figure S7: ^{1}H NMR of *(E)*-1-([1,1'-biphenyl]-4-yl)-3-(pyridin-4-yl) prop-2-en-1-one (3c)

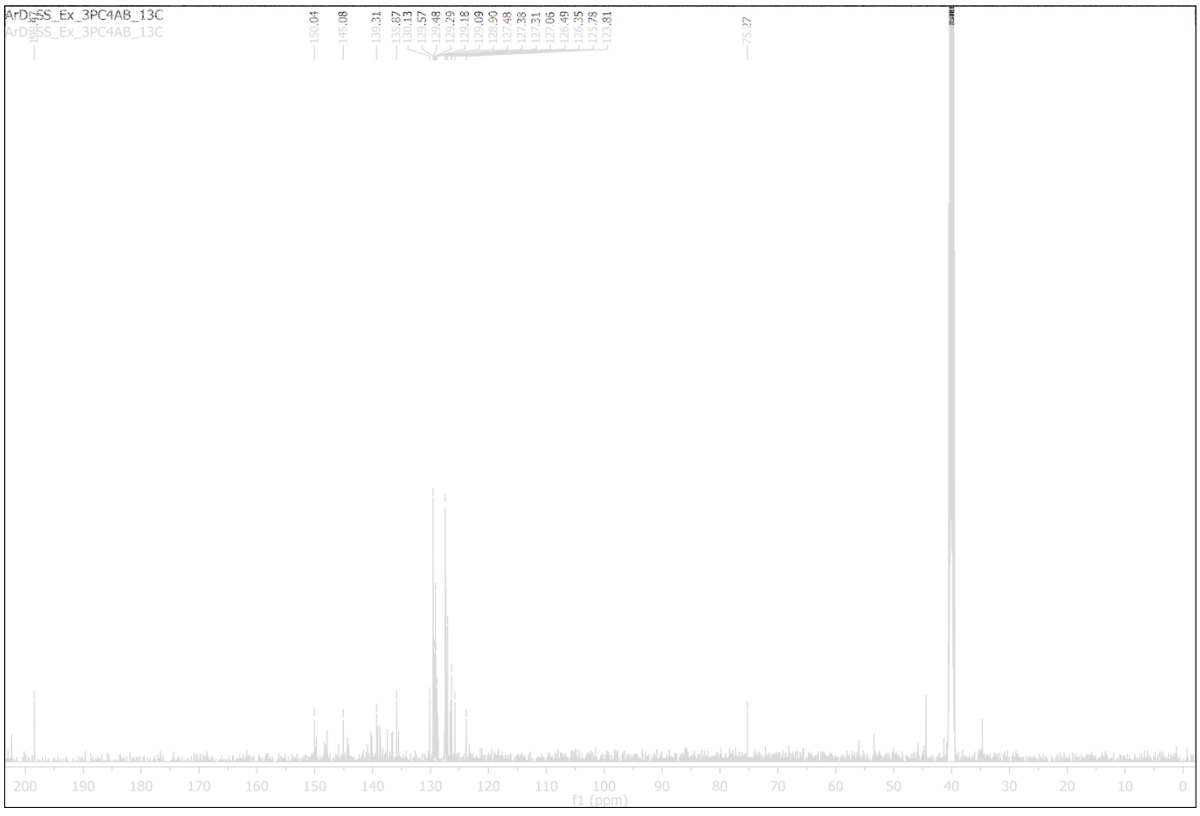

Figure S8: ^{13}C NMR of *(E)*-1-([1,1'-biphenyl]-4-yl)-3-(pyridin-4-yl) prop-2-en-1-one (3c)

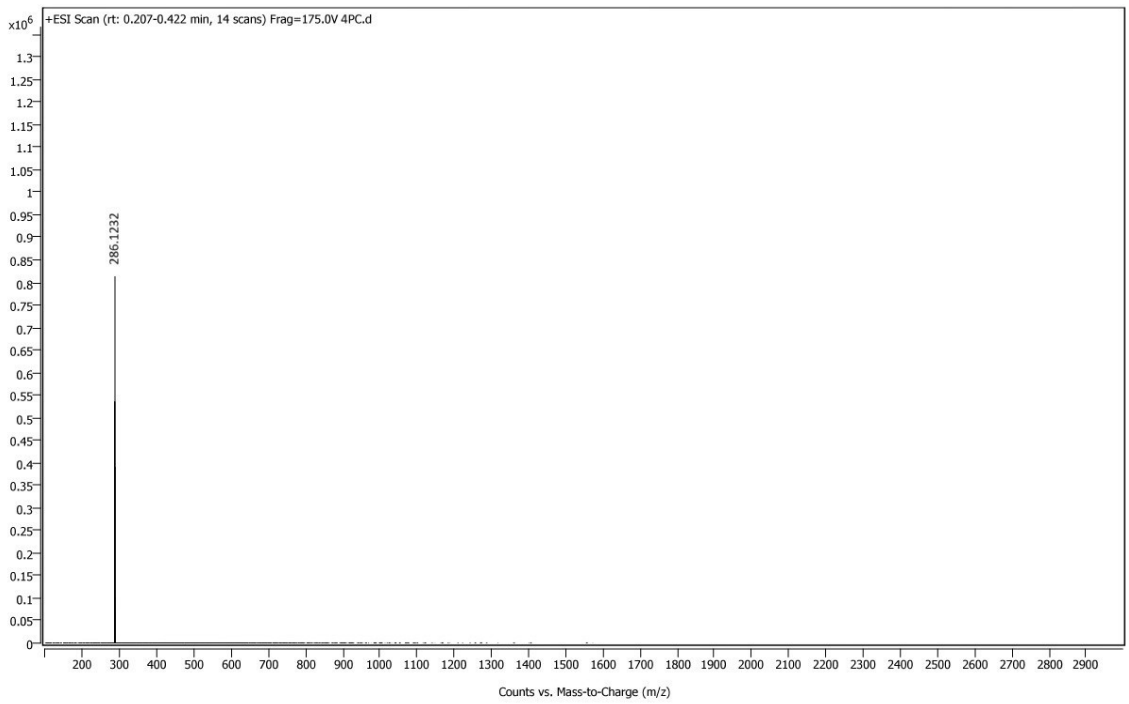

Figure S₉: HRMS of *(E)*-1-([1,1'-biphenyl]-4-yl)-3-(pyridin-4-yl) prop-2-en-1-one (3c)

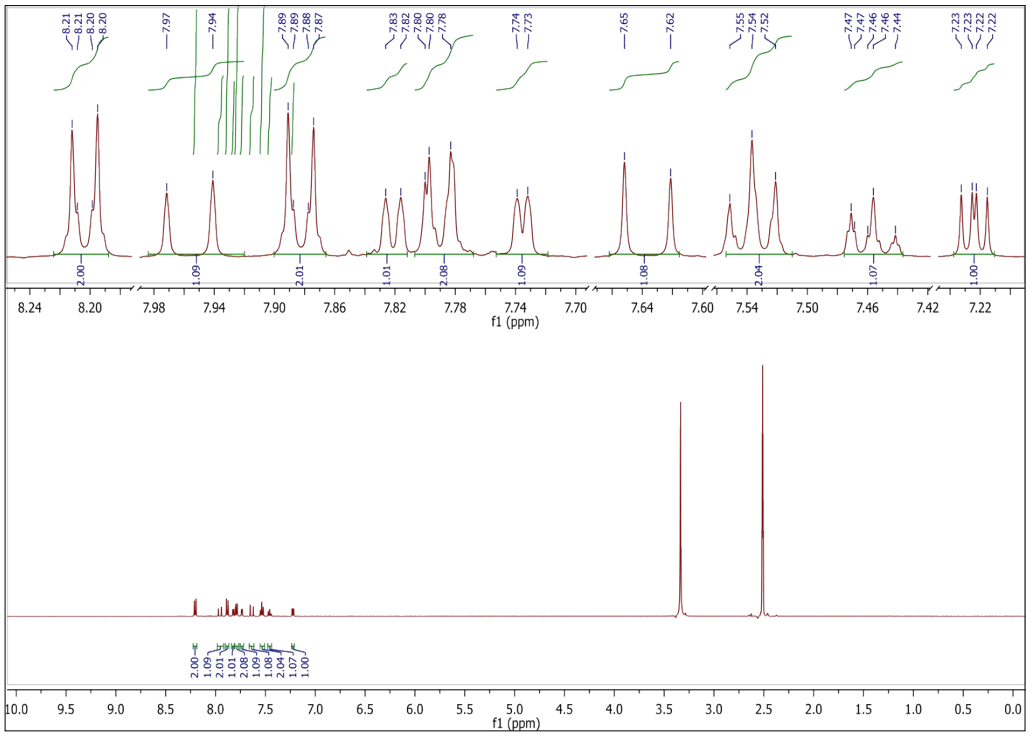

Figure S₁₀: ^{1}H NMR of *(E)*-1-([1,1'-biphenyl]-4-yl)-3-(thiophen-2-yl) prop-2-en-1-one (3d)

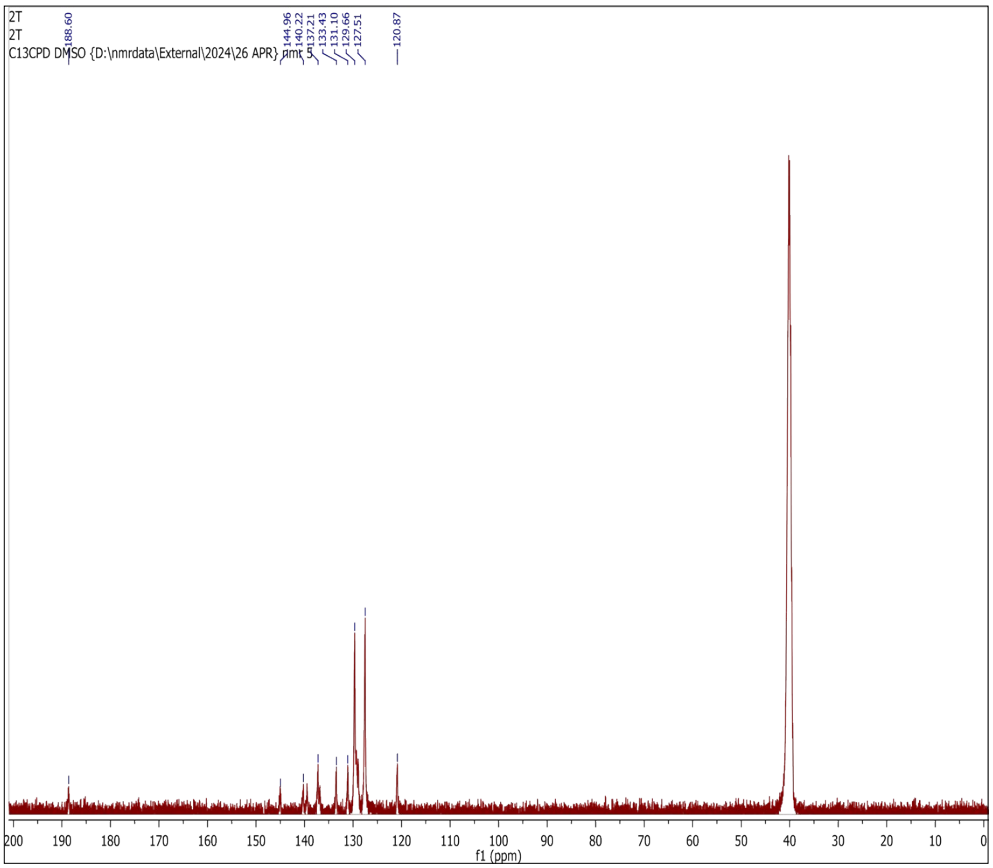

Figure S$_{11}$: ^{13}C NMR of *(E)*-1-([1,1'-biphenyl]-4-yl)-3-(thiophen-2-yl) prop-2-en-1-one (3d)

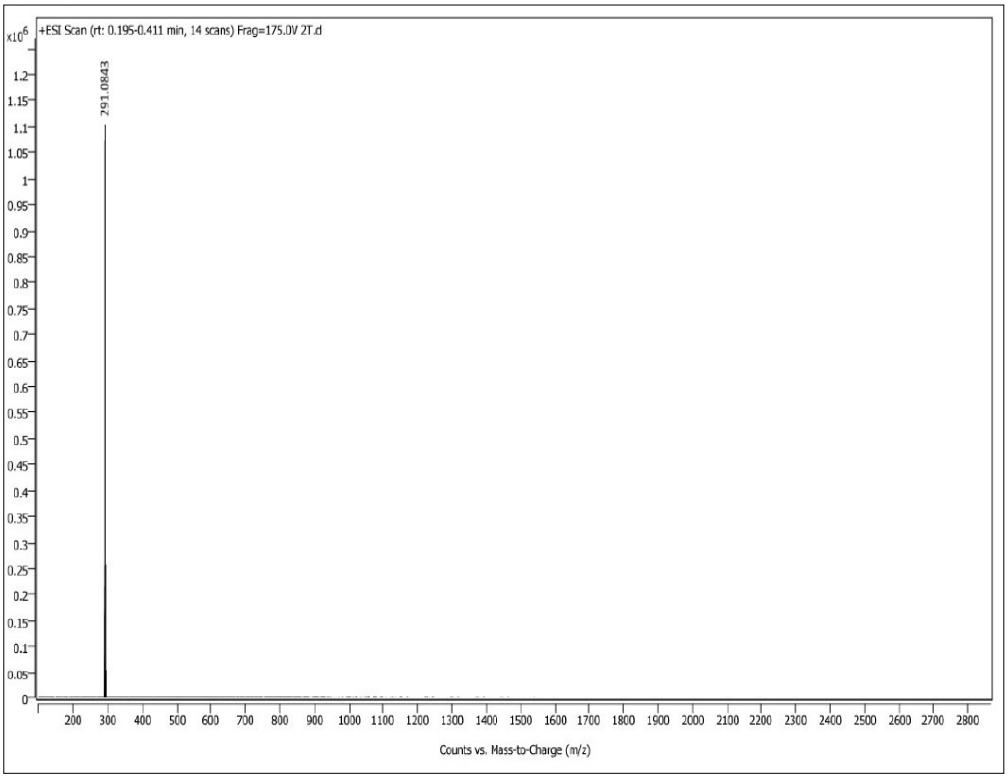

Figure S$_{12}$: HRMS of *(E)*-1-([1,1'-biphenyl]-4-yl)-3-(thiophen-2-yl) prop-2-en-1-one (3d)

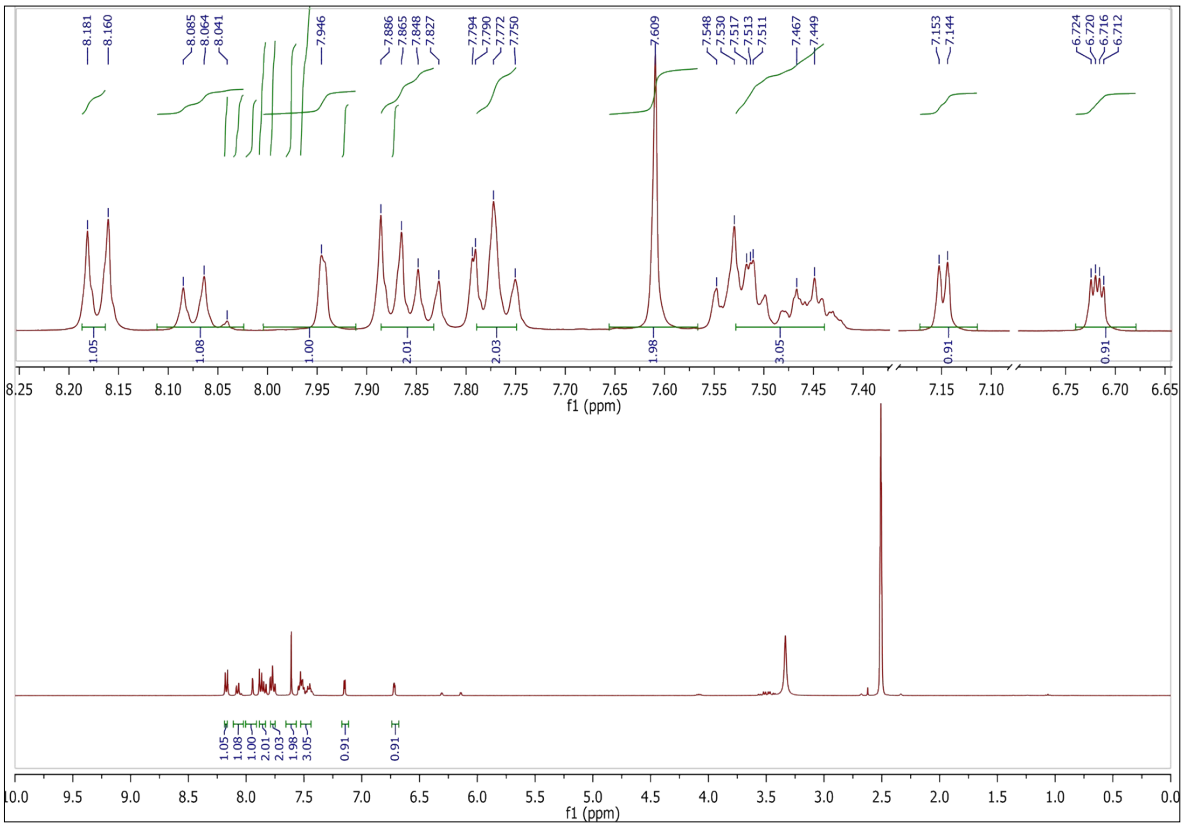

Figure S$_{13}$: ^{1}H NMR of *(E)*-1-([1,1'-biphenyl]-4-yl)-3-(furan-2-yl) prop-2-en-1-one (3e)

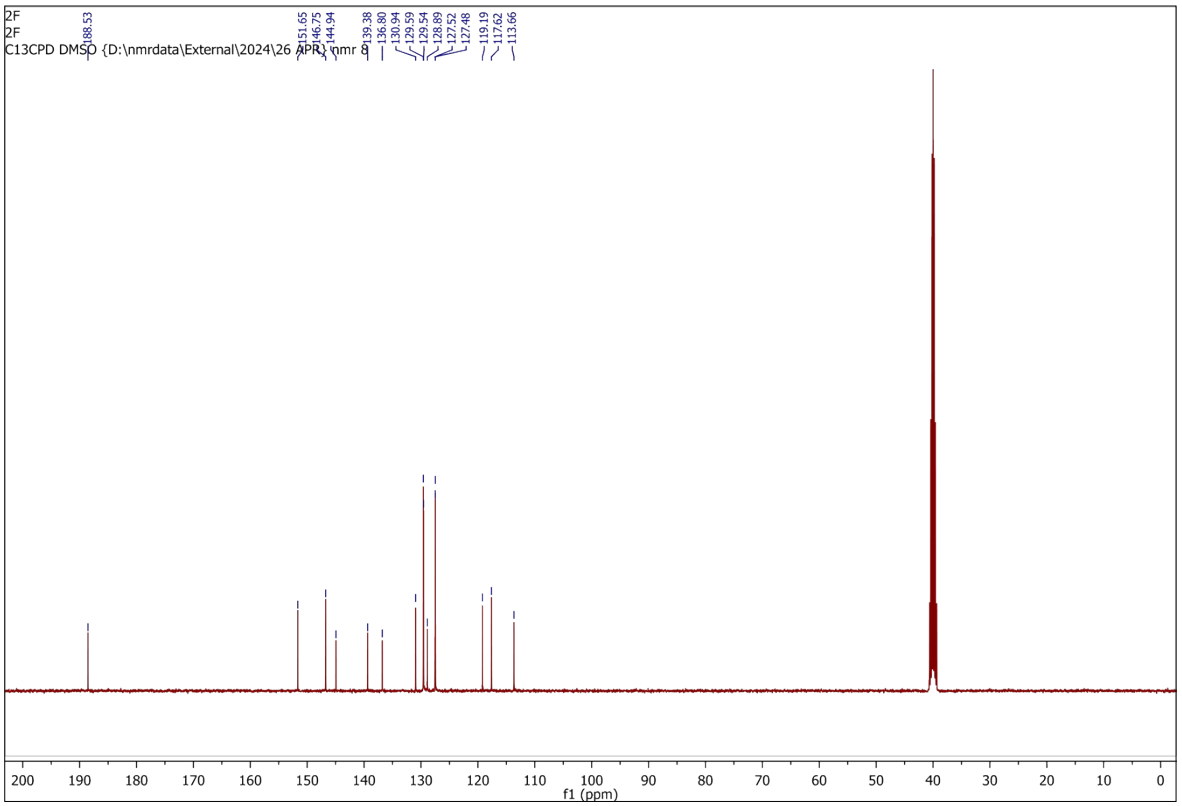

Figure S$_{14}$: ^{13}C NMR of *(E)*-1-([1,1'-biphenyl]-4-yl)-3-(furan-2-yl) prop-2-en-1-one (3e)

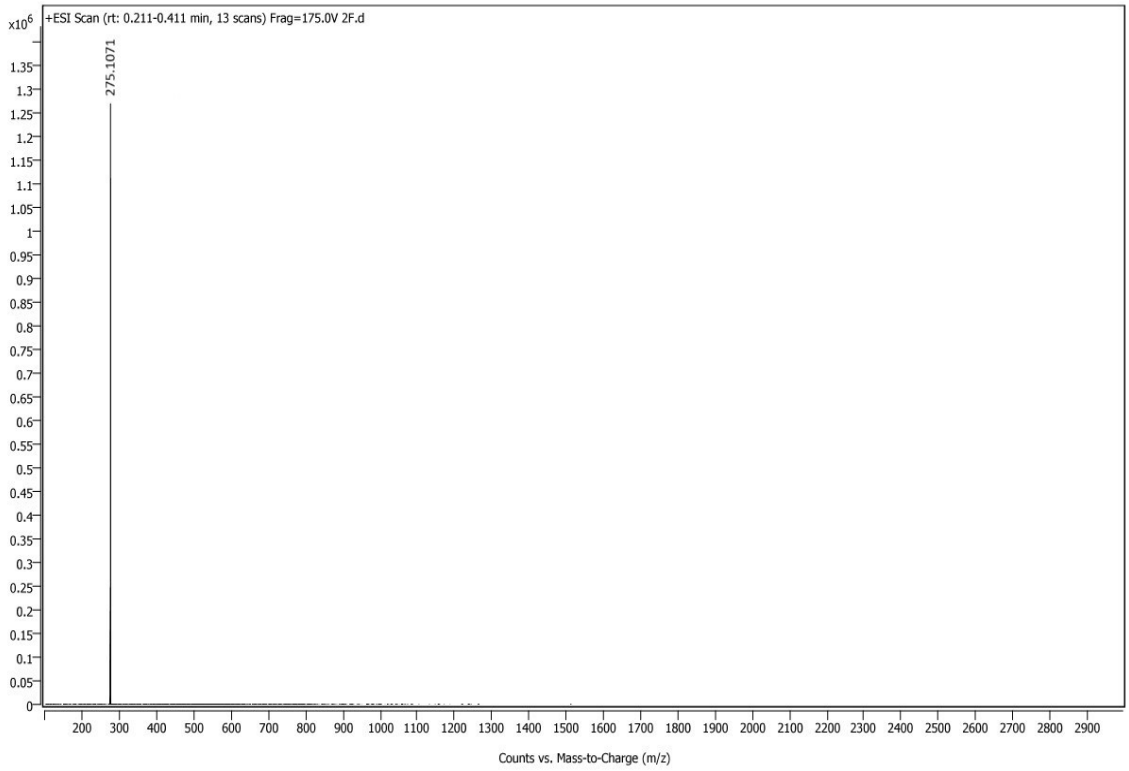

Figure S$_{15}$: HRMS of *(E)*-1-([1,1'-biphenyl]-4-yl)-3-(furan-2-yl) prop-2-en-1-one (3e)

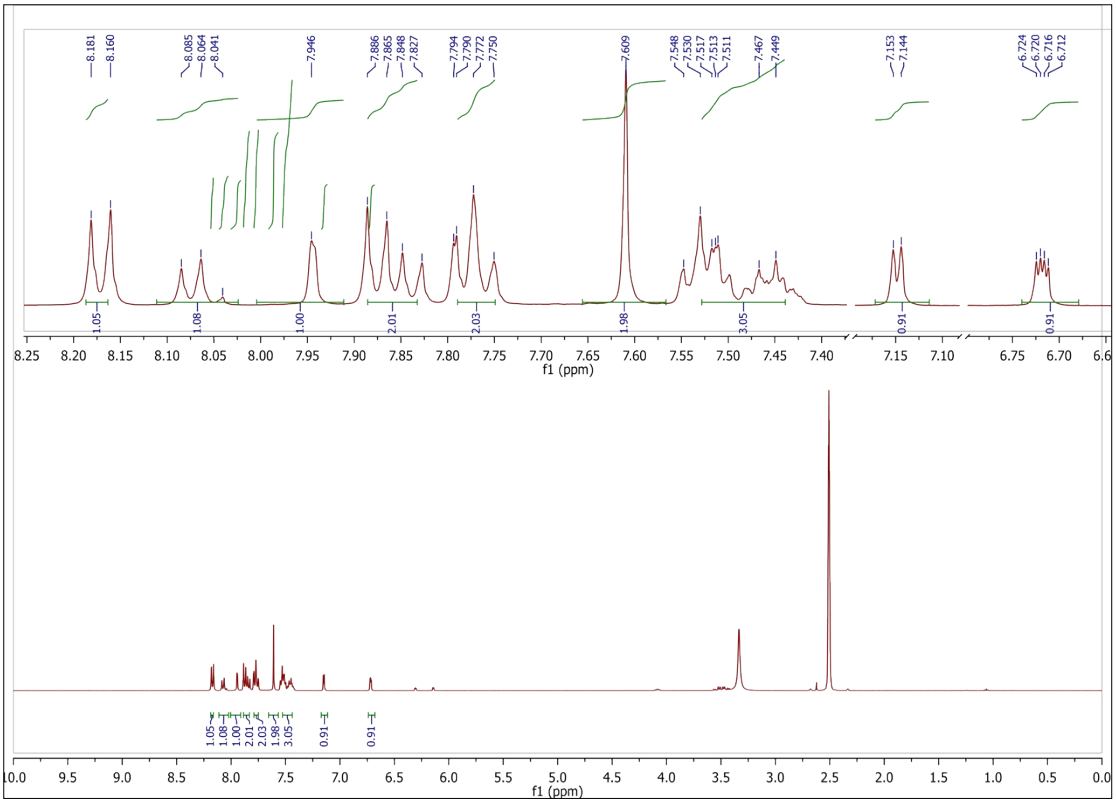

Figure S$_{16}$:^{1}H NMR of *(E)*-1-([1,1'-biphenyl]-4-yl)-3-(1H-imidazol-2-yl) prop-2-en-1-one (3f)

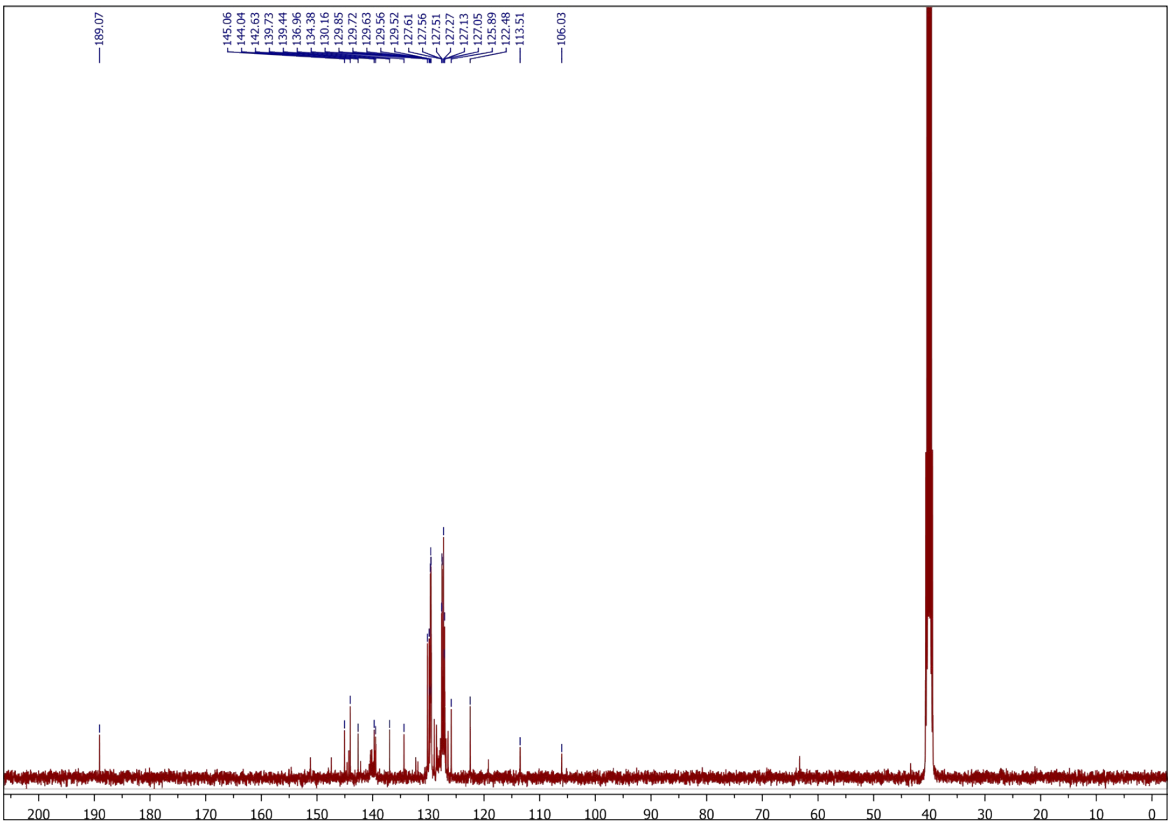

Figure S$_{17}$: ^{13}C NMR of *(E)*-1-([1,1'-biphenyl]-4-yl)-3-(1H-imidazol-2-yl) prop-2-en-1-one (3f)

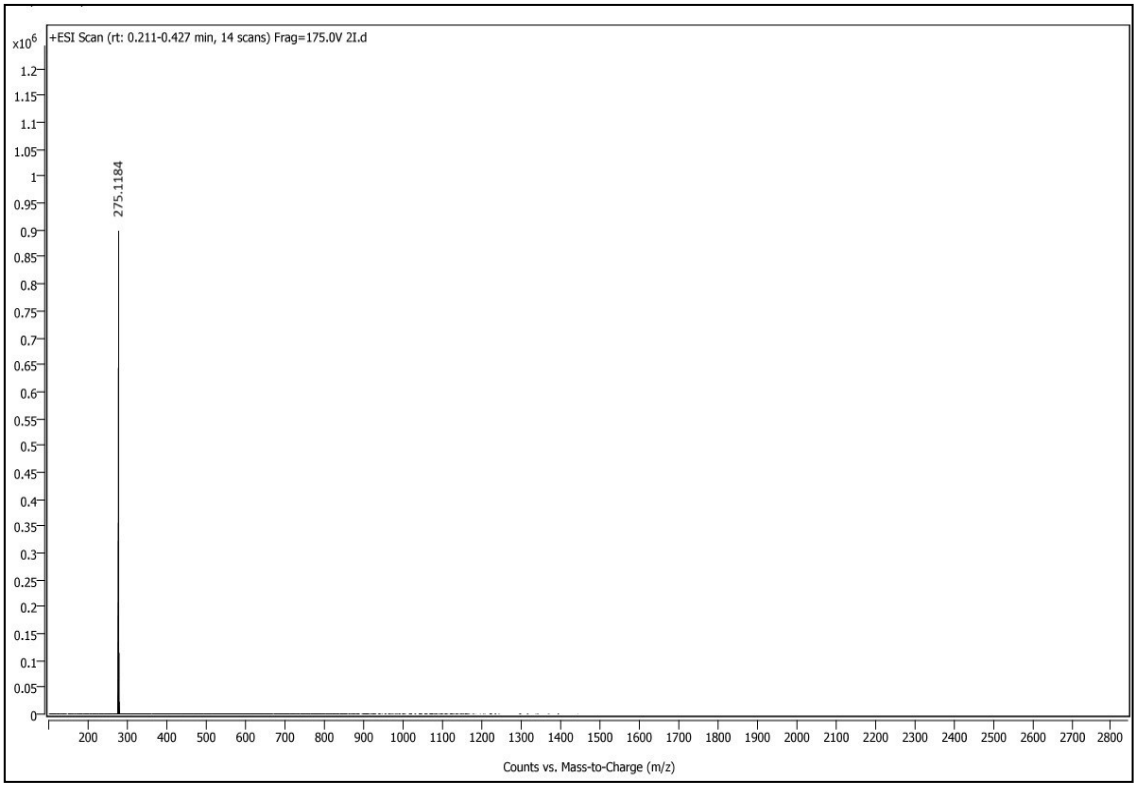

Figure S$_{18}$: HRMS of *(E)*-1-([1,1'-biphenyl]-4-yl)-3-(1H-imidazol-2-yl) prop-2-en-1-one (3f)

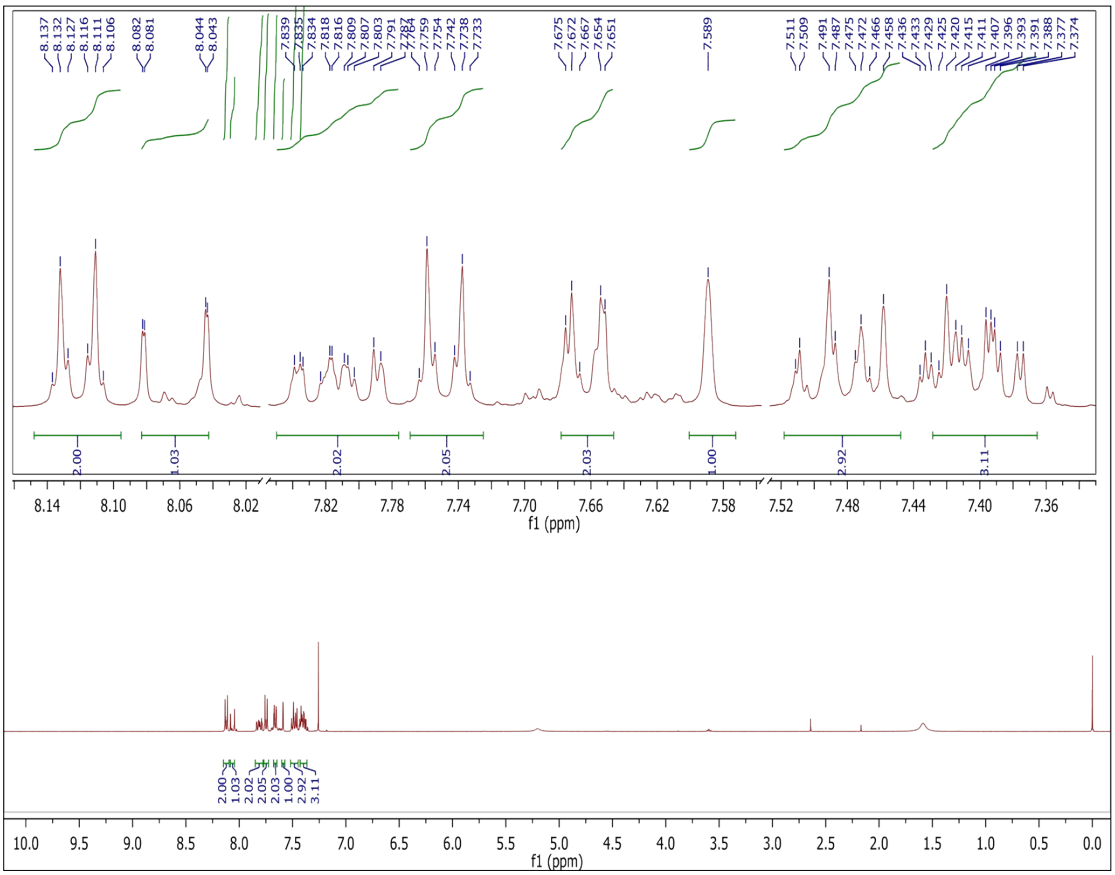

Figure S$_{19}$: ^{1}H NMR of *(E)*-1-([1,1'-biphenyl]-4-yl)-3-(benzo[b]thiophen-2-yl) prop-2-en-1-one (3g)

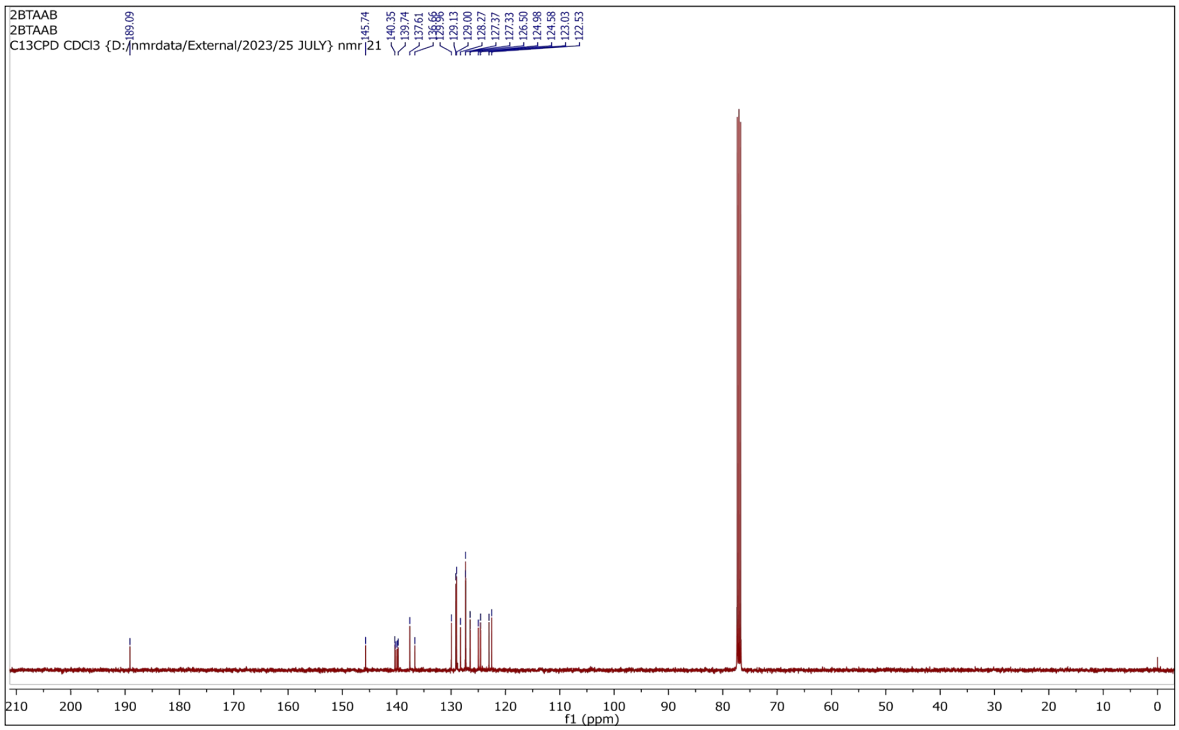

Figure S$_{20}$: ^{13}C NMR of *(E)*-1-([1,1'-biphenyl]-4-yl)-3-(benzo[b]thiophen-2-yl) prop-2-en-1-one (3g)

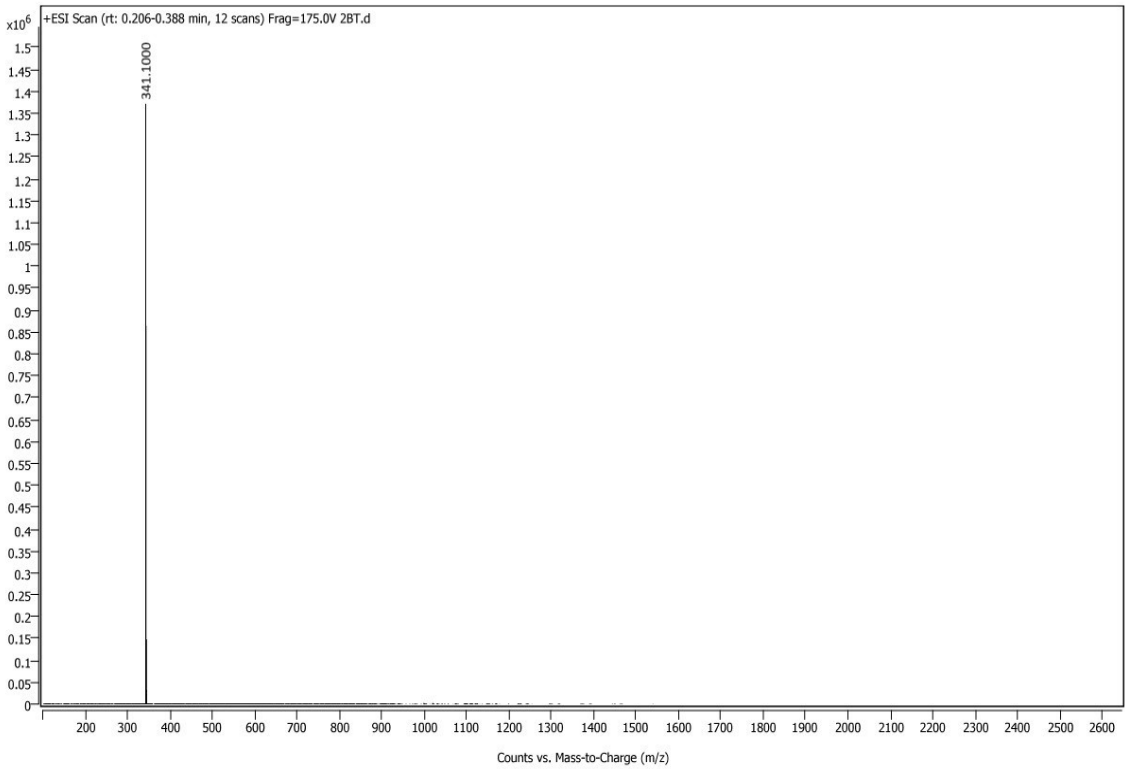

Figure S$_{21}$: HRMS of *(E)*-1-([1,1'-biphenyl]-4-yl)-3-(benzo[b]thiophen-2-yl) prop-2-en-1-one (3g)

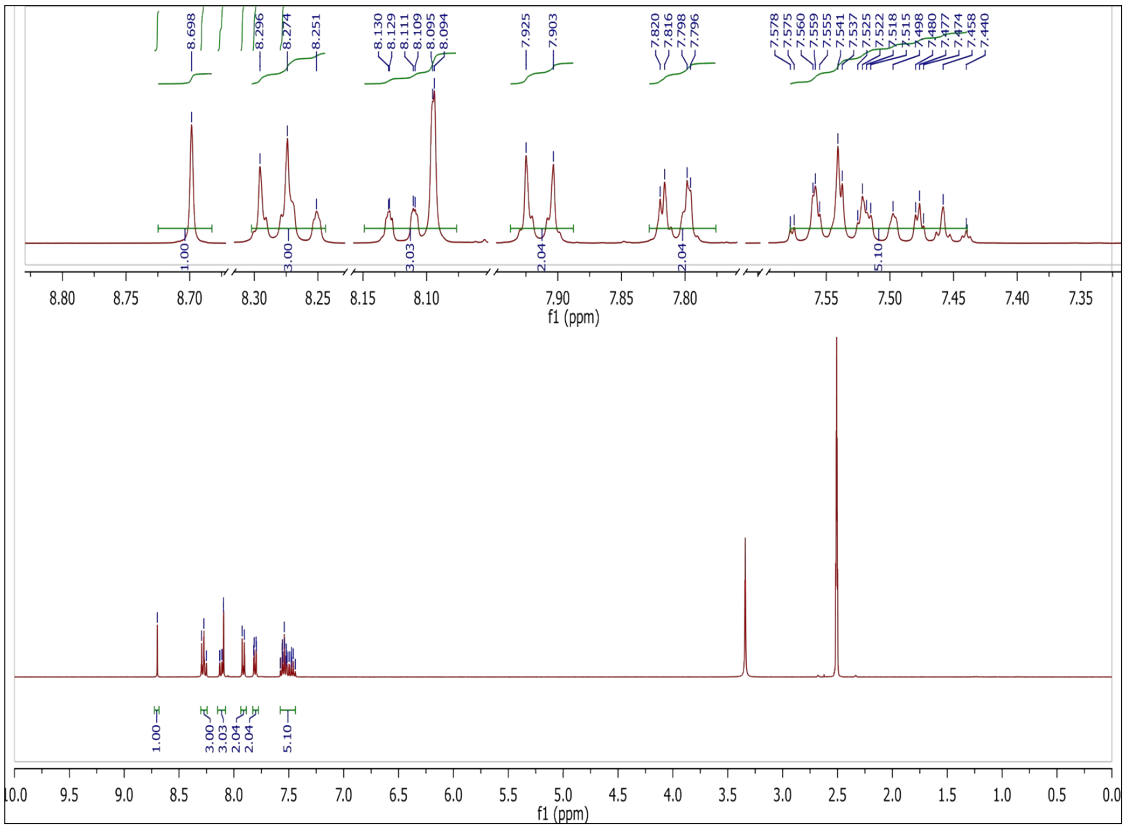

Figure S$_{22}$:^{1}H NMR of *(E)*-1-([1,1'-biphenyl]-4-yl)-3-(benzo[b]thiophen-3-yl) prop-2-en-1-one (3h)

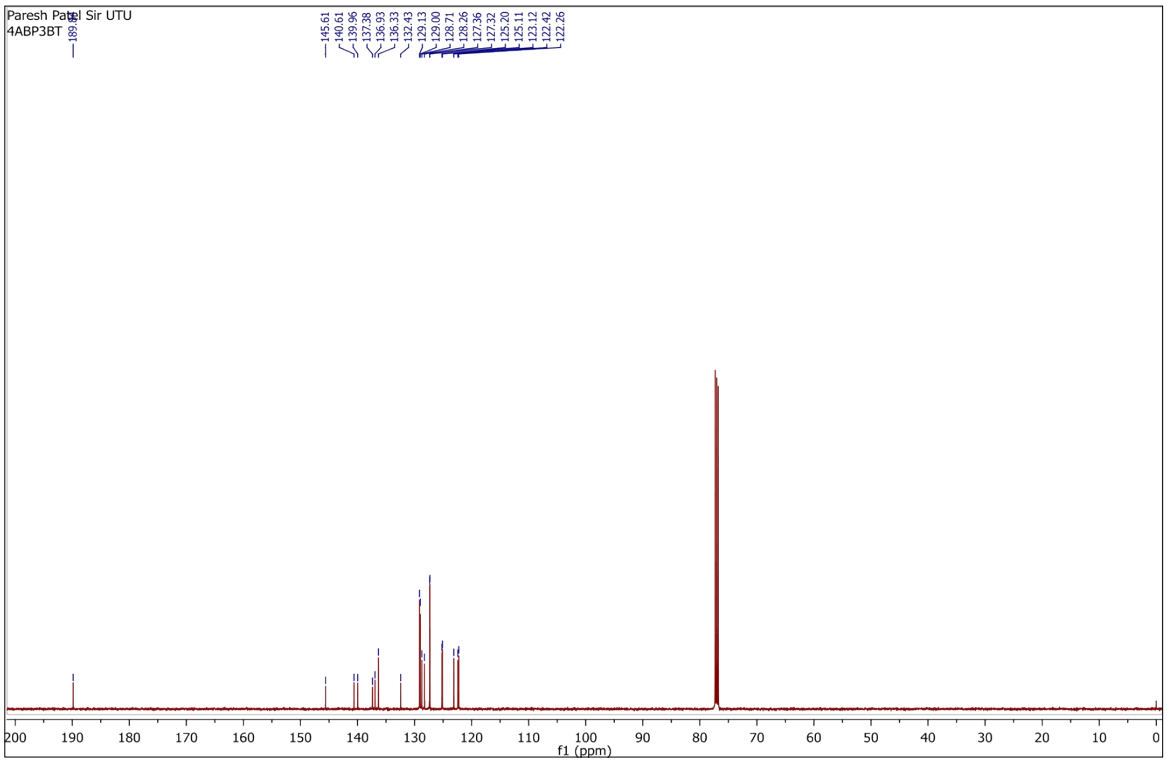

Figure S$_{23}$:^{13}C NMR of *(E)*-1-([1,1'-biphenyl]-4-yl)-3-(benzo[b]thiophen-3-yl) prop-2-en-1-one (3h)

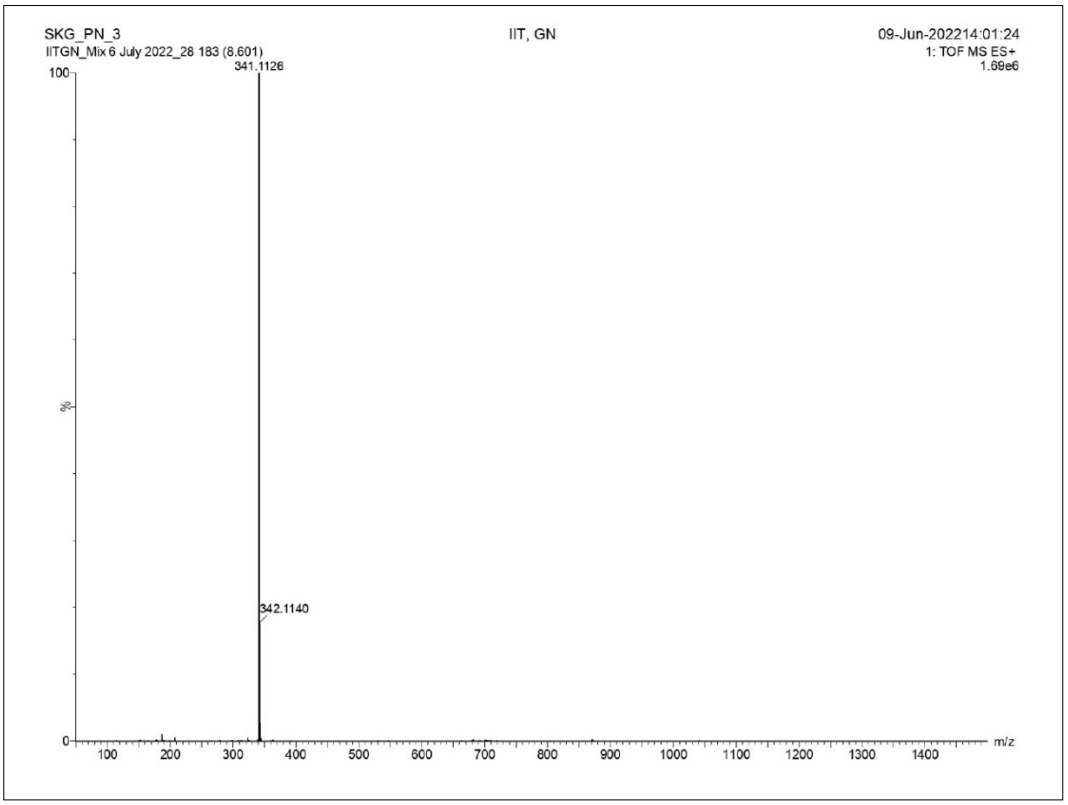

Figure S$_{24}$: HRMS of *(E)*-1-([1,1'-biphenyl]-4-yl)-3-(benzo[b]thiophen-3-yl) prop-2-en-1-one (3h)

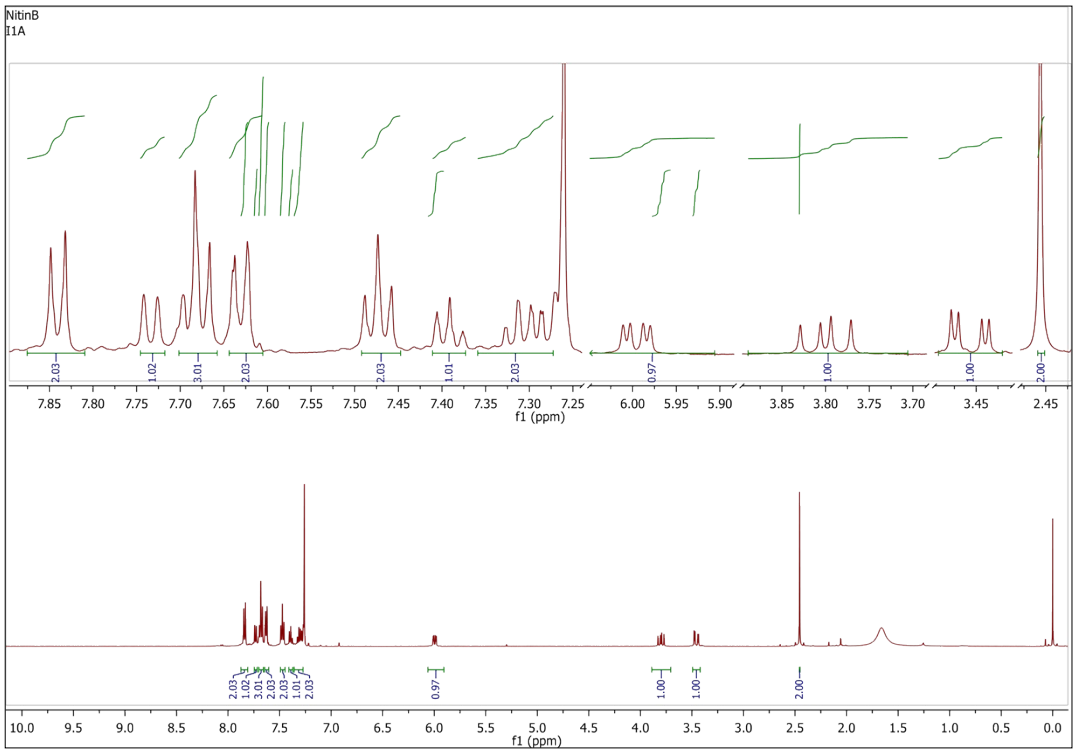

Figure S$_{25}$: ^{1}H NMR of 3-([1,1'-biphenyl]-4-yl)-5-(benzo[b]thiophen-2-yl)-4,5-dihydro-1H-pyraole(3g-NH_2NH_2)

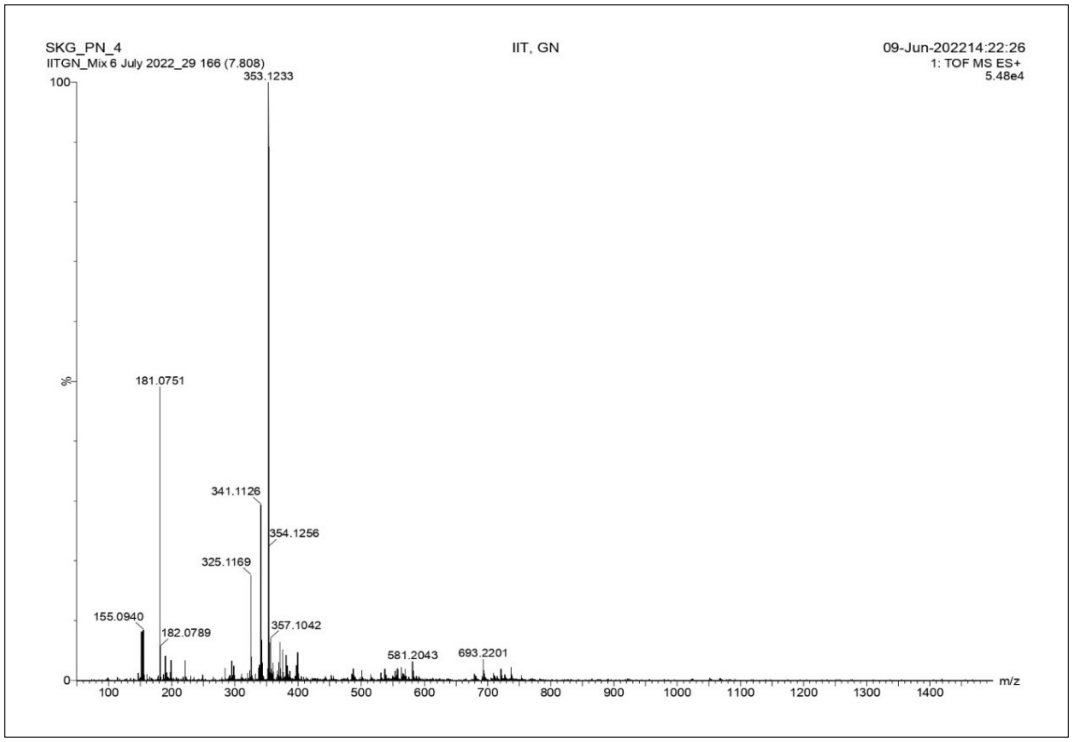

Figure S$_{26}$: HRMS of 3-([1,1'-biphenyl]-4-yl)-5-(benzo[b]thiophen-2-yl)-4,5-dihydro-1H-pyraole(3g-NH_2NH_2)

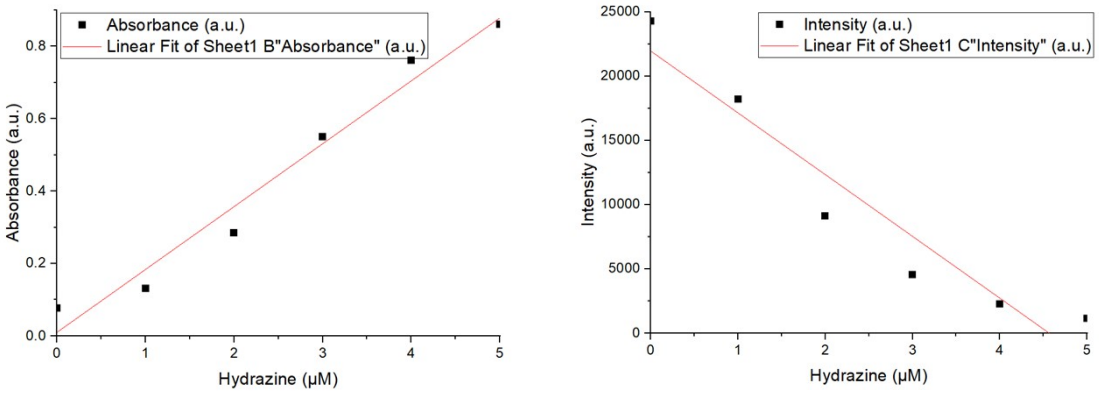

Equation	y = a + b*x	
Plot	Intensity (a.u.)	Absorbance (a.u.)
Weight	No Weighting	
Intercept	26932.49524± 3647.36	0.7224 ± 0.09197
Slope	10150.98857± 1204.68336	-0.15505 ± 0.03038
Residual Sum of Squares	1.01588E8	0.06459
Pearson's r	0.97297	-0.93108
R-Square (COD)	0.94667	0.8669
Adj. R-Square	0.93334	0.83363
LoD	0.11 µM	0.19 µM
LoQ	1.18 µM	1.95 µM

Figure S_{27}: Linear fitting curve of **(a)** the absorbance at 356 nm and **(b)** fluorescent intensities at 481 nm, toward concentration of N_2H_4 from 1.0 - 5.0 µM in 5.0 µM fluorochrome **3g**

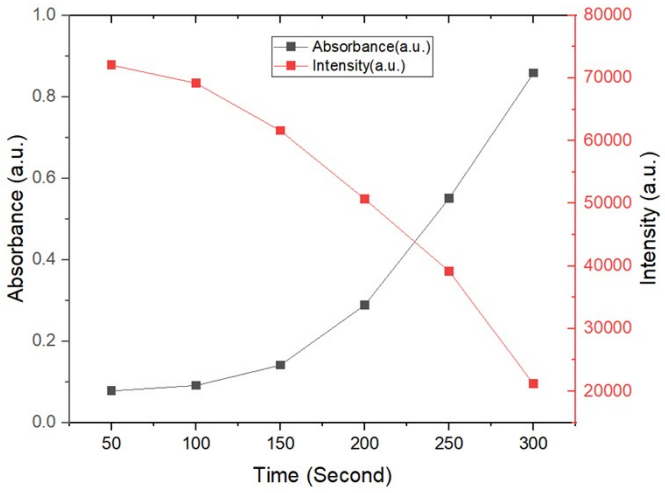

Figure S_{28}: The time course plot (time *vs* emission intensity and time *vs* absorbance) of 5.0 µM hydrazine detection by 5.0 µM fluorochrome **3g**

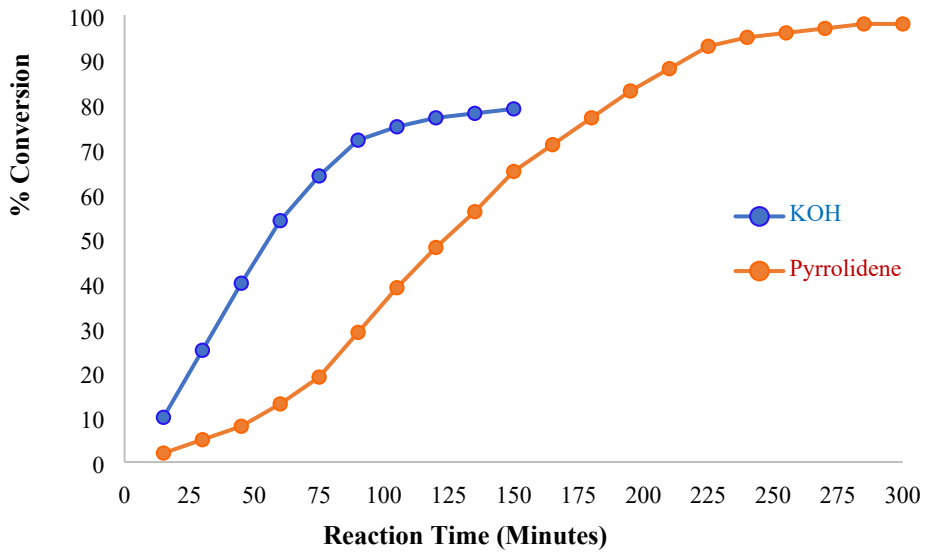

Figure S_{29}: % Conversion of fluorochrome **3a** under KOH and Pyrrolidine catalysed reactions

In case of KOH catalysed reaction, we were able to complete the reaction in shorter reaction time (~2 hrs) but with significantly low yield (~75 %) compare to pyrrolidine catalysed reactions. The reaction was completed almost 70 % in first 90 minutes, however to attend ~80 % completion it took 120 minutes and after that there was no further improvements (**Fig. S29**). The lower isolated yield could be because of significant solubility of obtained chalcone in ethanolic KOH. These results show pyrrolidine as an efficient catalyst for reaction under minder reaction conditions with high isolated yield (~95 %) in prolonged reaction time (~5 hrs). Here the reaction was slow during first 60 minutes and it was having good conversion rate between 60 to 220 minutes. However, after that the reaction was almost steady.

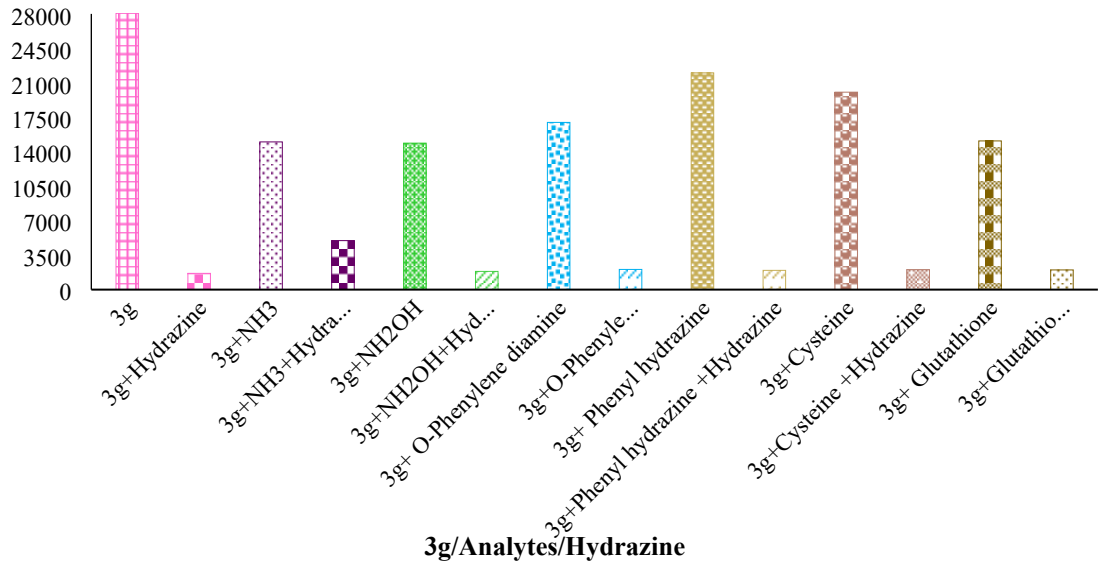

Figure S_{30}: Selective preference of **3g** (5µM; 481 nm) for hydrazine among different analytes

Table S1. Results for the determination of hydrazine in real samples of water and soil

*1gm soil was added to the solution prepared in water with different concentrations of hydrazine and 5 µM fluorochrome **3g**

Sample	Hydrazine added (µM)	Hydrazine detected (µM)	Recovery (%)	RSD (%)
Tap water	2	1.89	94.5	0.0234
	4	3.98	99.5	0.0416
	6	6.02	100.3	0.0253
River water	2	1.76	88.5	0.0354
	4	3.84	96.0	0.0412
	6	5.92	98.6	0.0511
Mineral water	2	1.97	98.5	0.0147
	4	4.01	100.2	0.0158
	6	6.03	100.5	0.0201
Clay soil 1gm*	2	1.79	89.5	0.0247
	4	3.82	95.5	0.0198
	6	5.90	98.3	0.0214
Field Soil 1gm*	2	1.68	84.0	0.0387
	4	3.56	89.0	0.0421
	6	5.62	93.6	0.0587
Sandy Soil 1gm*	2	1.85	92.5	0.0178
	4	3.93	98.2	0.0219
	6	5.87	97.8	0.0184

Table S2. Comparison with other reported fluorochrome

Sr. No.	Probe	Sensing mechanism	LoD µM	Linear range µM	Ref.
1.	Probe 1	Schiff-base reaction	0.022	0-1	1
2.	Probe 1	Michael addition reaction	0.019	0-0.05	2
3.	DCM-LX	Nucleophilic substitution reaction	0.007	0-20	3
4.	CyOS		7.800	10-160	4
5.	CI-DCV		0.086	0-10	5
6.	Probe 1	Hydrolysis reaction	0.370	0-200	6
7.	Probe 2		0.490	0-200	
8.	Probe 5		0.057	2-16	7
9.	Probe 1	Addition-cyclization reaction	3.800	0-500	8
10.	Probe 1		0.083	0-8	9
11.	PLS 3e		0.11	0-5	10
12.	fluorochrome 3g		0.110	0-8	This work

No.	Probe	LOD (µM)	Sensing method	Response time	Solvent (v/v)	Application	Ref
1	Coumarin	0.003	Ratiometric/ICT	40 min	Acetate buffer/DMSO (1:9)	TLC plates, Hela cells	11
2	Coumarin-Dichlorofluorescein	4.74×10^{-8}	Ratiometric/ FRET	30 min	PBS/DMSO (19:1)	Living cells	12
3	Fluorescein	9.0×10^{-8}	OFF-ON/-	10 min	Tris buffer/ DMSO (1:1)	Tap Water	13
4	BODIPY	1.4×10^{-6}	OFF-ON/PET	20 min	H_2O/DMSO (1:9)	-----	14
5	Phenanthro [9,10-d] imidazole	1.5 ppb	OFF-ON/-	40 min	HEPES buffer	HepG2 cells, invitro enzymatic assay	15
6	Benzothiazole	2.2 ppb	Ratiometric/ ESIPT	60 s	H_2O/CH_3CN (3:2)	Candidaalbicans cells	16
7	Pyridomethene - BF_2 derivative	----	OFF-ON/ICT	30 min	HEPES/CH_3CN (7:3)	HeLa cells, mice	17
8	Rhodol	0.83 ppb	OFF-ON/-	5 min	HEPES/EtoH (7:3)	Paper strips,	18

						HepG2 cells	
9	Quinoline	------	Ratiometric/ICT	1 min	$H2O/CH_3CN$ (3:7)	Filter paper, CHO cells	19
10	Flouro chrome 3g	1.1	ICT/FRET	15 min	methanol	Soil, water, filter paper	This work

Table S3. Quantum yield values of all the prepared FC and standard Rhodamine 101

Sr. No.	**FC**	**Solvent**	**Quantum Yield**	**Emission Range (nm)**
1	3a	Methanol	0.39	520 to 650
2	3b	Methanol	0.42	570 to 660
3	3c	Methanol	0.58	570 to 650
4	3d	Methanol	0.62	565 to 655
5	3e	Methanol	0.79	500 to 660
6	3f	Methanol	0.67	560 to 650
7	3g	Methanol	0.28	555 to 665
8	Rhodamine 101	Ethanol + 0.01% HCl	1.0	600 to 650

Table S4. Fluorochrome **3g** energy, wavelength and their oscillation with along major contribution in solvent and Gas phase

No.	Energy (cm^{-1})	Wavelength (nm)	Osc. Strength	Symmetry	Major contribs
1	27221.4	367.358034488	0.6757	Singlet-A	H-1->LUMO (20%), HOMO->LUMO (73%)
2	27432.71872	364.528215452	0.0567	Singlet-A	H-4->LUMO (40%), H-3->LUMO (18%), H-1->LUMO (16%), HOMO->LUMO (13%)
3	28594.16512	349.721698746	0.2302	Singlet-A	H-2->LUMO (72%), H-1->LUMO (21%)
4	30246.0	330.622231039	0.1433	Singlet-A	H-4->LUMO (14%), H-2->LUMO (23%), H-1->LUMO (41%), HOMO->LUMO (10%)
5	33688.39808	296.838097681	0.0049	Singlet-A	H-5->LUMO (87%)
6	34381.23312	290.856350763	0.0024	Singlet-A	H-4->LUMO (31%), H-3->LUMO (66%)
7	35425.72832	282.280717271	0.1869	Singlet-A	HOMO->L+1 (92%)
8	37371.9576	267.580310002	0.3608	Singlet-A	H-1->L+1 (78%)
9	37780.07696	264.689773147	0.0109	Singlet-A	H-2->L+1 (78%)
10	39435.13808	253.580955637	0.0551	Singlet-A	H-6->LUMO (88%)
11	39719.0472	251.768375753	0.0239	Singlet-A	H-4->L+1 (36%), H-3->L+1 (42%), H-1->L+2 (10%)
12	40301.38352	248.130439369	0.0088	Singlet-A	H-7->LUMO (34%), H-5->L+1 (17%), H-1->L+2 (12%), HOMO->L+3 (11%)
13	40437.69216	247.294033508	0.0354	Singlet-A	H-7->LUMO (21%), H-5->L+1 (15%), H-4->L+1 (22%), H-1->L+2 (10%)
14	40573.19424	246.468146946	0.0051	Singlet-A	H-5->L+1 (25%), H-4->L+1 (14%), H-3->L+1 (24%), H-1->L+4 (14%)
15	41306.35728	242.093485325	0.0789	Singlet-A	H-8->LUMO (10%), H-7->LUMO (22%), HOMO->L+3 (28%), HOMO->L+5 (14%)

Table S5. Intermediate energy, wavelength and their oscillation with along major contribution in solvent and Gas phase

No.	Energy (cm^{-1})	Wavelength (nm)	Osc. Strength	Symmetry	Major contribs
1	26074.47168	383.516878989	0.4291	Singlet-A	HOMO->LUMO (91%)
2	29916.11696	334.267980479	0.4449	Singlet-A	H-1->LUMO (90%)
3	30978.35648	322.806021244	0.2949	Singlet-A	H-2->LUMO (91%)
4	31497.78112	317.482681142	0.3587	Singlet-A	HOMO->L+1 (91%)
5	34152.97664	292.800247118	0.0512	Singlet-A	H-6->LUMO (10%), H-3->LUMO (80%)

6	35529.77456	281.454079679	0.002	Singlet-A	H-5->LUMO (67%), H-4->LUMO (12%)
7	36950.93328	270.629159059	0.0845	Singlet-A	H-1->L+1 (31%), HOMO->L+2 (35%), HOMO->L+3 (10%)
8	37149.34704	269.183735295	0.197	Singlet-A	H-1->L+1 (60%), HOMO->L+3 (12%)
9	37419.54464	267.240023795	0.0004	Singlet-A	H-5->LUMO (11%), H-4->LUMO (81%)
10	37957.52016	263.452405685	0.0066	Singlet-A	H-6->LUMO (24%), HOMO->L+2 (13%), HOMO->L+3 (28%)
11	38047.85488	262.826906577	0.0833	Singlet-A	H-6->LUMO (43%), HOMO->L+2 (14%), HOMO->L+3 (17%)
12	39061.7008	256.005237744	0.0045	Singlet-A	HOMO->L+4 (56%)
13	39189.94384	255.167500133	0.0593	Singlet-A	H-2->L+1 (77%)
14	40553.8368	246.585792839	0.0243	Singlet-A	H-3->L+1 (10%), HOMO->L+5 (40%), HOMO->L+6 (18%)
15	40769.99488	245.278421776	0.0141	Singlet-A	H-5->L+1 (19%), H-1->L+2 (14%), HOMO->L+6 (22%)

Table S6. Fluorochrome 3g-Hydrazine energy, wavelength and their oscillation with along major contribution in solvent and Gas phase

No.	**Energy (cm-1)**	**Wavelength (nm)**	**Osc. Strength**	**Symmetry**	**Major contribs**
1	29599.13888	337.847666466	0.8215	Singlet-A	HOMO->LUMO (92%)
2	33265.76064	300.609389583	0.0263	Singlet-A	H-1->LUMO (46%), HOMO->L+1 (50%)
3	34148.94384	292.834825196	0.2361	Singlet-A	H-1->LUMO (51%), HOMO->L+1 (41%)
4	36330.68864	275.249393126	0.0036	Singlet-A	H-5->LUMO (28%), HOMO->L+2 (56%)
5	36782.36224	271.869433908	0.0024	Singlet-A	H-2->LUMO (61%), H-1->L+1 (18%)
6	37964.7792	263.402032376	0.1359	Singlet-A	H-3->LUMO (17%), H-

					2->LUMO (30%), H-1->L+1 (35%)
7	38373.70512	260.595112427	0.0106	Singlet-A	H-4->LUMO (29%), H-3->LUMO (11%), HOMO->L+4 (33%)
8	38482.59072	259.857764587	0.0553	Singlet-A	H-3->LUMO (56%), H-1->L+1 (11%)
9	39427.87904	253.627642254	0.055	Singlet-A	H-2->L+1 (13%), H-1->L+1 (22%), H-1->L+3 (13%), HOMO->L+3 (44%)
10	40202.9832	248.737760336	0.0195	Singlet-A	H-2->L+1 (29%), H-1->L+3 (17%), HOMO->L+3 (45%)
11	40740.15216	245.458091583	0.0117	Singlet-A	H-4->LUMO (50%), HOMO->L+2 (21%), HOMO->L+4 (18%)
12	41282.16048	242.235384092	0.0067	Singlet-A	H-5->LUMO (12%), HOMO->L+4 (16%), HOMO->L+5 (51%)
13	41942.73312	238.420323525	0.0266	Singlet-A	H-5->LUMO (12%), H-1->L+6 (18%), HOMO->L+6 (52%)
14	42350.85248	236.122755846	0.0685	Singlet-A	H-5->LUMO (24%), H-1->L+6 (12%), HOMO->L+5 (22%), HOMO->L+6 (14%)
15	43023.52352	232.430986164	0.0024	Singlet-A	H-1->L+6 (60%), HOMO->L+6 (26%)

Table S7. Optimized coordinates of the fluorochrome **3g, Intermediate** and **3g-N_2H_4** molecules

fluorochrome **3g**

8	0.356324000	3.773575000	0.211142000
6	0.232462000	2.563307000	0.035638000
6	-1.128869000	2.004705000	-0.133888000

1	-1.865688000	2.753797000	-0.415630000
6	-1.510933000	0.745617000	0.171952000
1	-0.764567000	0.033696000	0.517209000
6	-2.855410000	0.218788000	0.119304000
6	-3.230570000	-1.054941000	0.462713000
16	-4.238521000	1.182238000	-0.424957000
6	-4.630561000	-1.313193000	0.307135000
1	-2.520947000	-1.793492000	0.820571000
6	-5.325305000	-0.174395000	-0.176105000
6	-6.704035000	-0.200936000	-0.402719000
1	-7.225756000	0.676225000	-0.772051000
6	-7.392984000	-1.380886000	-0.142507000
1	-8.464634000	-1.421022000	-0.312076000
6	-6.721684000	-2.520954000	0.337215000
1	-7.283395000	-3.429169000	0.532563000
6	-5.353662000	-2.494783000	0.562363000
1	-4.836261000	-3.374918000	0.933135000
6	1.445656000	1.681378000	0.016227000
6	1.536894000	0.505960000	-0.744207000
6	2.574200000	2.102137000	0.736722000
6	2.716962000	-0.233264000	-0.767933000
1	0.698233000	0.189482000	-1.355154000
6	3.743062000	1.352989000	0.727476000
1	2.508244000	3.022898000	1.306555000
6	3.840003000	0.167775000	-0.025711000
1	2.779996000	-1.116184000	-1.396492000
1	4.589717000	1.675590000	1.325563000
6	5.093119000	-0.627307000	-0.043645000
6	6.348483000	0.004168000	-0.026183000
6	5.056950000	-2.031652000	-0.079588000
6	7.525175000	-0.742221000	-0.044805000

1	6.400973000	1.088644000	-0.025665000
6	6.233651000	-2.778106000	-0.097472000
1	4.098300000	-2.541470000	-0.066500000
6	7.473205000	-2.136622000	-0.080428000
1	8.484506000	-0.232938000	-0.040063000
1	6.181923000	-3.862896000	-0.116418000
1	8.390254000	-2.718034000	-0.094714000

Intermediate

6	0.245608000	2.396841000	0.023522000
6	-1.098990000	1.823535000	-0.105590000
1	-1.830289000	2.469143000	-0.592244000
6	-1.488712000	0.604444000	0.330263000
1	-0.767275000	-0.029074000	0.842279000
6	-2.807152000	0.026960000	0.204001000
6	-3.201860000	-1.192299000	0.691361000
16	-4.138468000	0.856626000	-0.623813000
6	-4.574278000	-1.512072000	0.430656000
1	-2.525601000	-1.848831000	1.228533000
6	-5.229992000	-0.479392000	-0.287354000
6	-6.574832000	-0.580174000	-0.651065000
1	-7.065192000	0.216587000	-1.201484000
6	-7.272608000	-1.728908000	-0.290319000
1	-8.318879000	-1.825780000	-0.563783000
6	-6.640688000	-2.763739000	0.422583000
1	-7.206685000	-3.650020000	0.692637000
6	-5.304667000	-2.663360000	0.782867000
1	-4.818214000	-3.463592000	1.333249000
6	1.466434000	1.546818000	0.009791000
6	1.527591000	0.337737000	-0.702116000
6	2.622142000	1.964168000	0.691934000
6	2.694254000	-0.421578000	-0.727899000

1	0.664535000	0.002549000	-1.267360000
6	3.785518000	1.205430000	0.663543000
1	2.588251000	2.892189000	1.251735000
6	3.848853000	-0.008085000	-0.044287000
1	2.720178000	-1.333253000	-1.317337000
1	4.651212000	1.539937000	1.227465000
6	5.089860000	-0.821394000	-0.066906000
6	6.354369000	-0.209444000	-0.113061000
6	5.035620000	-2.225657000	-0.043645000
6	7.520245000	-0.972711000	-0.134253000
1	6.420964000	0.873357000	-0.159372000
6	6.201226000	-2.989410000	-0.066517000
1	4.070986000	-2.720409000	0.018891000
6	7.449578000	-2.366577000	-0.111334000
1	8.485958000	-0.477193000	-0.178341000
1	6.134109000	-4.073357000	-0.040061000
1	8.358055000	-2.961369000	-0.128447000
7	0.445677000	3.678835000	0.129510000
7	-0.650026000	4.503839000	0.181261000
1	-1.437893000	4.156356000	0.724887000
1	-0.363397000	5.421212000	0.497318000

3g-N_2H_4

6	0.085750000	-1.657512000	0.029434000
6	0.987140000	-1.742012000	1.251485000
6	2.347289000	-2.078868000	0.600483000
6	3.251945000	-0.887047000	0.406120000
6	2.925892000	0.421789000	0.213652000
16	4.996961000	-1.152296000	0.295958000
6	4.060376000	1.273408000	-0.029711000
1	1.906049000	0.789438000	0.234548000
6	5.280247000	0.552312000	-0.019357000

6	6.509409000	1.183824000	-0.230583000
1	7.436277000	0.618920000	-0.218408000
6	6.515502000	2.555695000	-0.458568000
1	7.459478000	3.065307000	-0.626158000
6	5.315354000	3.289102000	-0.474974000
1	5.345395000	4.359221000	-0.656176000
6	4.096407000	2.660907000	-0.262813000
1	3.171226000	3.229965000	-0.277227000
6	-1.280790000	-1.132464000	0.021835000
6	-1.868583000	-0.622387000	1.190851000
6	-2.044640000	-1.119299000	-1.161271000
6	-3.165855000	-0.116770000	1.179122000
1	-1.315886000	-0.631490000	2.125380000
6	-3.335320000	-0.612638000	-1.168138000
1	-1.600409000	-1.505766000	-2.072081000
6	-3.928703000	-0.098237000	0.001487000
1	-3.603425000	0.243609000	2.105137000
1	-3.890867000	-0.589724000	-2.100830000
6	-5.310827000	0.440669000	-0.012447000
6	-6.309251000	-0.151505000	-0.805228000
6	-5.660473000	1.557965000	0.765600000
6	-7.607651000	0.354556000	-0.819799000
1	-6.070291000	-1.031883000	-1.394154000
6	-6.959216000	2.063265000	0.752393000
1	-4.899833000	2.049813000	1.364570000
6	-7.939285000	1.464258000	-0.040743000
1	-8.364167000	-0.125033000	-1.434356000
1	-7.203521000	2.932907000	1.355812000
1	-8.951104000	1.858489000	-0.051844000
7	0.645804000	-2.147312000	-1.027761000
7	1.889377000	-2.660661000	-0.701392000

1	2.535611000	-2.532378000	-1.474742000
1	2.879453000	-2.854284000	1.158233000
1	1.020761000	-0.825276000	1.844815000
1	0.659301000	-2.553367000	1.913250000

Table S8. The calculated energy and its Gibbs free values of reaction along with intermediate.

S. No.	Reactions	ΔE	ΔH	ΔG
1	**3g → Intermediate**	-2.66	-3.89	-2.79
2	**Intermediate → 3g-NH_2NH_2**	-8.68	-8.04	-6.66
3	**3g → 3g-NH_2NH_2**	-11.33	-11.93	-9.45

References:

1. J. L. Wang, H. Wang, S. X. Yang, H. Y. Tian, Y. G. Liu, Y. F. Hao, J. Zhang, B. G. Sun, A Fluorescent Probe for Sensitive Detection of Hydrazine and Its Application in Red Wine and Water, *Anal. Sci.*, 2018, **34**, 329-333.
2. H. Wang, X. Wu, F. Tao, S. X. Yang, H. Y. Tian, Y. G. Liu, B. G. Sun, A Highly Selective and Colorimetric Fluorescent Probe for Hydrazine Detection in Water Samples, *Anal. Sci.*, 2018, **34**, 1297-1302.
3. X. Yang, Y. Liu, Y. Wu, X. Ren, D. Zhang, Y. Ye, A NIR ratiometric probe for hydrazine "naked eye" detection and its imaging in living cell, *Sens. Actuators, B*, 2017, **253**, 488-494.
4. S. Wang, S. Ma, J. Zhang, M. She, P. Liu, S. Zhang, J. Li, A highly sensitive and selective near-infrared fluorescent probe for imaging hydrazine in living tissues and mice, *Sens. Actuators, B*, 2018, **261**, 418-424.
5. C. Liu, F. Wang, T. Xiao, B. Chi, Y. Wu, D. Zhu, X. Chen, The ESIPT fluorescent probes for N_2H_4 based on benzothiazole and their applications for gas sensing and bioimaging, *Sens. Actuators, B*, 2018, **256**, 55-62.
6. Y. Liu, D. Ren, J. Zhang, H. Li, X. F. Yang, A fluorescent probe for hydrazine based on a newly developed 1-indanone-fused coumarin scaffold, *Dyes Pigm.*, 2019, **162**, 112-119.
7. W. Z. Xu, W. Y. Liu, T. T. Zhou, Y. T. Yang, W. Li, A novel fluorescein-based "turn-on" probe for the detection of hydrazine and its application in living cells, *Spectrochim. Acta, Part A*, 2019, **193**, 324-329.

8. H. Wang, Y. N. Li, S. X. Yang, H. Y. Tian, Y. G. Liu, B. G. Sun, A dual-function fluorescent probe for discriminative detection of hydrogen sulfide and hydrazine, *J. Photochem. Photobiol., A*, 2019, **377**, 36-42.
9. Y. Li, X. Wu, S. Yang, S. Liang, H. Tian, B. Sun, A Natural Light Visible Colorimetric Responses Fluorescent Probe for Hydrazine Detection, *ANAL. SCI.,* 2020, **36**, 323-327.
10. D.V., Kasundra, S.N., Tandel, P. N., Patel, Biphenyl based photo luminescent sensor for real time hydrazine detection: Design, Synthesis, DFT and Single crystal XRD studies, *J. Mol. Structure* 2025, ***1330***, 141486.
11. M. Xing, K. Wang, X. Wu, S. Ma, D. Cao, R. Guan, Z. Liu, A coumarin chalcone ratiometric fluorescent probe for hydrazine based on deprotection, addition and subsequent cyclization mechanism, *Chem. Commun*., 2019, **55**, 14980.
12. Z. Zhang, Z. Zhuang, L.L. Song, X. Lin, S. Zhang, G. Zheng, F. Zhan, A FRET-based ratiometric fluorescent probe for hydrazine and its application in living cells, *J. Photochem. Photobiol. A Chem.* 2018, **358**, 10-16.
13. M.G. Choi, J.O. Moon, J. Bae, J.W. Lee, S.K. Chang, Hydrazine selective dual signaling chemodosimetric probe in physiological conditions and its application in live cells, *Org. Biomol. Chem.* 2013, **11**, 2961-2965.
14. B. Li, Z. He, H. Zhou, H. Zhang, W. Li, T. Cheng, G. Liu, Reaction based colorimetric and fluorescence probes for selective detection of hydrazine*, Dye. Pigments*, 2017, **146**, 300-304.
15. F. Ali, A.H. A, N. Taye, D.G. Mogare, S. Chattopadhyay, A. Das, Specific receptor for hydrazine: Mapping the: In situ release of hydrazine in live cells and in an in vitro enzymatic assay, *Chem. Commun*., 2016, **52**, 6166-6169.
16. S. Goswami, S. Das, K. Aich, B. Pakhira, S. Panja, S.K. Mukherjee, S. Sarkar, A chemodosimeter for the ratiometric detection of hydrazine based on return of ESIPT and its application in live-cell imaging, *Org. Lett.,* 2013, **15**, 5412-5415.
17. Z. Lu, X. Shi, Y. Ma, W. Fan, Y. Lu, Z. Wang, C. Fan, A simple two-output near infrared fluorescent probe for hydrazine detection in living cells and mice, *Sensors Actuators, B Chem*., 2018, **258**, 42-49.
18. K. Tiensomjitr, R. Noorat, S. Chomngam, K. Wechakorn, S. Prabpai, P. Kanjanasirirat, Y. Pewkliang, S. Borwornpinyo, P. Kongsaeree, *Spectrochim. Acta – Part A Mol. Biomol. Spectrosc*.,2018, **195**, 136-141.
19. S. Yu, S. Wang, H. Yu, Y. Feng, S. Zhang, M. Zhu, H. Yin, X. Meng, A ratiometric two-photon fluorescent probe for hydrazine and its applications, *Sensors Actuators, B Chem*., 2015**, 220**, 1338-1345.